Angular distributions for $\Lambda_b \to \Lambda_J^*(pK^-)J/\psi(\to \ell^+\ell^-)$ decays

Zhi-Peng Xing[1,*], Fei Huang,[2,†] and Wei Wang[2,‡]

[1]*Tsung-Dao Lee Institute, Shanghai Jiao Tong University, Shanghai 200240, China*
[2]*INPAC, Shanghai Key Laboratory for Particle Physics and Cosmology,*
Key Laboratory for Particle Astrophysics and Cosmology (MOE),
School of Physics and Astronomy, Shanghai Jiao-Tong University,
Shanghai 200240, People's Republic of China

We carry out an analysis of the multibody decay cascade $\Lambda_b \to \Lambda_J^* J/\psi \to pK^- J/\psi$ with the Λ_J^* resonance, including Λ_{1520}^*, Λ_{1600}^*, and Λ_{1800}^*, and J/ψ reconstructed by the lepton pair final state. Using the helicity amplitude technique, we derive a compact form for the angular distributions for the decay chain, from which one can extract various one-dimensional distributions. Using the $\Lambda_b \to \Lambda_J^*$ form factors from lattice QCD and quark model, we calculate the differential and integrated partial widths. Decay branching fractions are found as $\mathcal{B}(\Lambda_b \to \Lambda_J^*(pK)J/\psi(\ell^+\ell^-)) = (1.35 \pm 0.28) \times 10^{-5}$. In addition, we also explore forward-backward asymmetry and various polarizations. Results in this work will serve a calibration for the study of $b \to s\ell^+\ell^-$ decays in Λ_b decays in future and provide useful information toward the understanding of the properties of the Λ_J^* baryons.

I. INTRODUCTION

Multibody hadronic decays of heavy mesons and baryons are of special interest for various reasons. Compared to two-body hadronic decay, multibody decays typically have much richer phase spaces and thus can be used to explore various new phenomena. Since these decays might receive distinct resonating contributions, they provide a platform for the study of strong interactions and the examination of the beneath quantum field theory, i.e., quantum chromodynamics (QCD), in a versatile manner. In addition, in the past decades, many traditional and exotic hadron structures have been discovered in multibody decays of heavy mesons and baryons at different experimental facilities [1–5].

The main focus of this work is the $\Lambda_b \to pK^- J/\psi$ decay, which has been previously explored on the experimental side. This process plays a very important role in the search for exotic hadron states. In 2015, the LHCb Collaboration reported two exotic structures, $P_c(4380)$ and $P_c(4450)$, first observed in the $\Lambda_b^0 \to J/\psi pK^-$ process [4]. In

addition, a new narrow state $P_c(4312)$ and a two-peak structure of $P_c(4450)$ have been discovered by analyzing the $\Lambda_b^0 \to J/\psi pK^-$ data from the LHCb Collaboration [6]. While the P_c resonances give sizable contributions to the decay widths, the $\Lambda_b \to \Lambda_J^*(pK^-)J/\psi$ contributions are also likely significant. Thus, the identification of exotic hadrons and precise determinations of their properties strongly depends on the understanding of the dynamics in this decay process. Actually, the contribution from the P_c pentaquark is small in the low-invariant-mass range ($M_{pk} = 1.4$–1.8 GeV), while the $\Lambda_{1520,1600,1800}^*$ resonances occupy dominant contributions in this energy range [4]. In this work, we mainly focus on the Λ_J^* resonance contributions.

Another salient feature of the $\Lambda_b \to \Lambda_J^*(pK)J/\psi(\ell^+\ell^-)$ decay is the wealth of information carried by angular observables in terms of angular asymmetries that can be used to probe new physics beyond the standard model. Our process is the basis for flavor-changing neutral current (FCNC) processes, which are involved in the Wilson coefficient C_9^{eff} in Ref. [7]. The FCNC process of $b \to s\ell^+\ell^-$ is forbidden at the tree level and is thus sensitive to new physics beyond the standard model. Thus, the $B \to K\ell^+\ell^-$ and $B \to K^*\ell^+\ell^-$ have received great attention in the past decades and have provided very stringent constraints on new physics beyond the standard model [8–18]. Meanwhile, in these decays, the so-called flavor anomalies are also found [19–27]. For instance, LHCb has presented its latest measurement of the ratio of branching fractions [21,26],

[*]zpxing@sjtu.edu.cn
[†]fhuang@sjtu.edu.cn
[‡]wei.wang@sjtu.edu.cn

$$R_K \equiv \frac{\mathcal{B}(B \to K\mu^+\mu^-)}{\mathcal{B}(B \to Ke^+e^-)}$$

$$= 0.846^{+0.042+0.013}_{-0.039-0.012}, \qquad 1.1 < q^2 < 6 \text{ GeV}^2,$$

$$R_{K^*} \equiv \frac{\mathcal{B}(B \to K^*\mu^+\mu^-)}{\mathcal{B}(B \to K^*e^+e^-)}$$

$$= 0.69^{+0.11}_{-0.07} \pm 0.05, \qquad 1.1 < q^2 < 6 \text{ GeV}^2, \qquad (1)$$

which has the 3.1σ and 2.8σ tension with the SM prediction, respectively. To further examine the implication of these observations, more experimental and theoretical analyses are called for. The Λ_b is a spin-1/2 hadron and has more polarization degrees of freedom than the B meson, and thus it is presumable that the baryonic decay $\Lambda_b \to \Lambda^*_J(\to pK^-)\ell^+\ell^-$ provides complementary information. In this regard, a detailed analysis of $\Lambda_b \to \Lambda^*_J J/\psi(\to \ell^+\ell^-)$ can provide a valuable benchmark.

The focus of this paper is the angular distributions for $\Lambda_b \to \Lambda^*_J(\to pK^-)J/\psi(\to \ell^+\ell^-)$, where Λ^*_J can decay into the pK^- final state. The angular distributions for Λ_b four-body decays with resonances depend on the different spin-parity of the Λ^*_J resonance and the interference between them. Based on the relevant experimental data [4], we find the resonances Λ^*_{1405}, Λ^*_{1520}, Λ^*_{1600}, Λ^*_{1800}, and Λ^*_{1810} give main contributions compared to other resonances, especially for Λ^*_{1670} with tiny contributions and Λ^*_{1690} with small integrated width. Since the Λ^*_J will decay into pK, the Λ^*_J mass should be above $m_K + m_p$ and thereby resonances like the Λ^*_{1405} are not allowed. In addition, the Λ^*_{1810} is very close to Λ^*_{1800} and will be treated together in the following. Therefore, we only consider three resonances Λ^*_{1520}, Λ^*_{1600}, and Λ^*_{1800} in our work. The spin-parity quantum numbers, masses, and decay widths of these resonances are shown in Table I.

The rest of this paper is organized as follows. In Sec. II, we give the theoretical framework for the $\Lambda_b \to \Lambda^*_J J/\psi$ with the Λ^*_J having different quantum numbers. The helicity amplitude is adopted to derive the angular distributions. In Sec. III, we make use of $\Lambda_b \to \Lambda^*_J$ from lattice QCD calculation and a quark model and calculate the differential decay widths. Angular distribution variables are also explored in this section and, in particular, the forward-backward asymmetry and polarizations are predicted. A brief summary will be presented in the last section. Some calculation details are collected in the Appendices.

TABLE I. The spin-party, masses, and decay width of resonances Λ^*_{1520}, Λ^*_{1600}, and Λ^*_{1800} [28].

Resonance	J^P	Mass (MeV)	Γ (MeV)
Λ^*_{1520}	$\frac{3}{2}^-$	1519.42 ± 0.19	15.73 ± 0.26
Λ^*_{1600}	$\frac{1}{2}^+$	~ 1600	~ 200
Λ^*_{1800}	$\frac{1}{2}^-$	~ 1800	~ 200

II. HELICITY AMPLITUDES

The decay kinematics for $\Lambda_b \to \Lambda^*_J(pK)J/\psi(\ell^+\ell^-)$ is shown in Fig. 1. In the Λ_b baryon rest frame, the Λ^*_J moves along the z axis. The $\theta(\theta_\Lambda)$ is defined as the angle between negative (positive) z axis and the moving direction of ℓ^- (p) in the J/ψ (Λ^*_J) rest frame. The ϕ is the angle between the Λ^*_J and J/ψ cascade decay planes.

Decay amplitude for the four-body decays can be divided into Lorentz-invariant hadronic part and leptonic matrix elements,

$$i\mathcal{M}(\Lambda_b \to \Lambda^*_J(pK)J/\psi(\ell^+\ell^-))$$

$$= \sum_{\Lambda^*_J} \sum_{s_{\Lambda^*_J} s_{J/\psi}} i\mathcal{M}(J/\psi \to \ell^+\ell^-)\frac{i}{q^2 - m^2_{J/\psi} + im_{J/\psi}\Gamma_{J/\psi}}$$

$$\times i\mathcal{M}(\Lambda_b \to \Lambda^*_J J/\psi)$$

$$\times \frac{i}{p^2_{\Lambda^*_J} - m^2_{\Lambda^*_J} + im_{\Lambda^*_J}\Gamma_{\Lambda^*_J}} i\mathcal{M}(\Lambda^*_J \to pK), \qquad (2)$$

with the J/ψ momentum $q^\mu = p^\mu_{\ell^+} + p^\mu_{\ell^-}$ and the Λ^*_J momentum $p^\mu_{\Lambda^*_J} = p^\mu_p + p^\mu_K$. In the above expression, a resonance approximation has been adopted for the production of pK^- and the lepton pair.

Since the individual parts with a specific polarization are Lorentz invariant, they can be calculated in different reference frames. The $\mathcal{M}(\Lambda_b \to \Lambda^*_J J/\psi)$ is induced by the $b \to sc\bar{c}$ transition, whose effective Hamiltonian is

$$\mathcal{H}_{\text{eff}}(b \to sc\bar{c}) = \frac{G_F}{\sqrt{2}}(V_{cb}V^*_{cs}(C_1O_1 + C_2O_2)), \quad (3)$$

with

$$O_1 = [\bar{c}_\alpha\gamma^\mu(1-\gamma_5)b_\beta][\bar{s}_\beta\gamma_\mu(1-\gamma_5)c_\alpha],$$

$$O_2 = [\bar{c}_\alpha\gamma^\mu(1-\gamma_5)b_\alpha][\bar{s}_\beta\gamma_\mu(1-\gamma_5)c_\beta]. \quad (4)$$
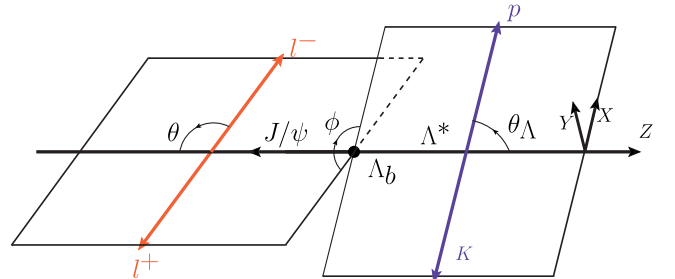
FIG. 1. The kinematics for the $\Lambda_b \to \Lambda^*_J(pK)J/\psi(\ell^+\ell^-)$ decay. In the Λ_b baryon rest frame, the Λ^*_J moves along the z axis. The $\theta(\theta_\Lambda)$ is defined as the angle between the negative (positive) z axis and the moving direction of ℓ^- (p) in the J/ψ (Λ^*_J) rest frame. The ϕ is the angle between the Λ^*_J and J/ψ cascade decay planes.

The G_F and V_{cb}, V_{cs} are the Fermi coupling constant and the Cabibbo-Kobayashi-Maskawa matrix element, respectively. O_i is the low-energy effective operator and C_i is the corresponding Wilson coefficient obtained by integrating out high-energy contributions. Applying the Fierz transformation and adopting the factorization ansatz, one can write the $\Lambda_b \to \Lambda_J^* J/\psi$ amplitude as

$$
\begin{aligned}
\mathcal{M}(\Lambda_b \to \Lambda_J^* J/\psi) = \frac{G_F}{\sqrt{2}} V_{cb} V_{cs}^* a_2 f_{J/\psi} m_{J/\psi} \\
\times \langle \Lambda_J^* | \bar{s} \gamma^\mu (1 - \gamma_5) b | \Lambda_b \rangle \epsilon_\mu^*(s_{J/\psi}), \\
a_2 = C_1 + C_2/N_c,
\end{aligned} \tag{5}
$$

with $m_{J/\psi} = 3.097$ GeV, $m_{\Lambda_b} = 5.619$ GeV, $V_{cs} = 0.975$, $V_{cb} = 0.041$, and $f_{J/\psi} = 0.405$ GeV. The $f_{J/\psi}$ and N_c are the decay constant of J/ψ and the color number for quarks, respectively. The Wilson coefficients at m_b scale are used as $C_1(m_b) = -0.248$ and $C_2(m_b) = 1.107$ [29].

The leptonic decay amplitude of J/ψ can be calculated with an effective Hamiltonian,

$$
\begin{aligned}
i\mathcal{M}(J/\psi \to \ell^+ \ell^-) \\
= \langle \ell^+(s_+) \ell^-(s_-) | -igF^{\mu\nu} F'_{\mu\nu} | J/\psi(s_{J/\psi}) \rangle \\
= 2ieg \times \bar{u}(s_-) \gamma^\mu v(s_+) \epsilon_\mu(s_{J/\psi}) \\
= 2ieg \times L_{s_-,s_+}^{s_{J/\psi}}(\theta, \phi),
\end{aligned} \tag{6}
$$

where $s_\pm$ and $s_{J/\psi}$ are the helicity of the $\ell^\pm$ and J/ψ, respectively. The $F_{\mu\nu} = \partial_\mu A_\nu - \partial_\nu A_\mu$ is the electromagnetic field strength tensor and $F'_{\mu\nu} = \partial^\mu A_{J/\psi}^\nu - \partial^\nu A_{J/\psi}^\mu$ characterizes the J/ψ. The explicit results for $L_{s_-,s_+}^{s_{J/\psi}}(\theta, \phi)$ are given in the Appendix A. The coupling constant g can be determined from the J/ψ leptonic decay width as follows:

$$
g^2 = \frac{3\Gamma(J/\psi \to \ell^+ \ell^-) m_{J/\psi}^2}{4\alpha_{em}(m_{J/\psi}^2 + 2m_\ell^2)\sqrt{m_{J/\psi}^2 - 4m_\ell^2}}. \tag{7}
$$

The hadron decay $\Lambda_J^* \to pK^-$ is parametrized as

$$
\begin{aligned}
i\mathcal{M}(\Lambda_J^* \to pK) = \mathcal{A}_J \times (D_{s_{\Lambda_J^*}, s_p}^{J_{\Lambda_J^*}}(\phi_\Lambda, \theta_\Lambda))^*, \\
J = 1520, 1600, 1800,
\end{aligned} \tag{8}
$$

where $J_{\Lambda_J^*}$ is the total spin of the Λ_J^*, and $s_{\Lambda_J^*}$ and s_p are the helicities, respectively. The $D_{s_{\Lambda_J^*}, s_p}^{J_{\Lambda_J^*}}(\phi_\Lambda, \theta_\Lambda)$ is the Wigner function [28], whose explicit expression is also given in Appendix A. It should be noticed that the ϕ_Λ is the angle from the $\Lambda_J^* pK^-$ plane and the x–z plane and can be chosen as zero in the calculation. Equation (8) applies to the distribution for any pertinent resonance, and in this analysis we consider the Λ_{1520}^*, Λ_{1600}^*, and Λ_{1800}^*. Using the two-body decay process $\Lambda_J^* \to pK$, one can extract the coupling strength $\mathcal{A}_J$ as

$$
\mathcal{A}_J = \sqrt{\Gamma(\Lambda_J^* \to pK)16\pi m_{\Lambda_J^*}^2/|\vec{p}_p|}, \quad J = 1520,
$$

$$
\mathcal{A}_J = \sqrt{\Gamma(\Lambda_J^* \to pK)8\pi m_{\Lambda_J^*}^2/|\vec{p}_p|}, \quad J = 1600, 1800. \tag{9}
$$

Then the decay amplitude of the $\Lambda_b \to \Lambda_J^*(pK)J/\psi(\ell^+ \ell^-)$ process is calculated as

$$
\begin{aligned}
&i\mathcal{M}(\Lambda_b \to \Lambda_J^*(pK)J/\psi(\ell^+ \ell^-)) \\
&= \frac{ge}{q^2 - m_{J/\psi}^2 + im_{J/\psi}\Gamma_{J/\psi}} L_{s_-,s_+}^{s_{J/\psi}}(\theta, \phi) \\
&\times \frac{1}{M_{pK}^2 - m_{\Lambda_J^*}^2 + im_{\Lambda_J^*}\Gamma_{\Lambda_J^*}} \mathcal{A}_J D_{s_{\Lambda^*}, s_p}^{*J_{\Lambda_J^*}}(\phi_\Lambda = 0, \theta_\Lambda) \\
&\times i\mathcal{M}(\Lambda_b \to \Lambda_J^* J/\psi).
\end{aligned} \tag{10}
$$

For the sake of simplicity, one can introduce the abbreviation $\mathcal{A}_{s_p, s_{J/\psi}}^{s_{\Lambda_b}}(\theta_\Lambda)$ for the hadronic part,

$$
\begin{aligned}
\mathcal{A}_{s_p, s_{J/\psi}}^{s_{\Lambda_b}}(\theta_\Lambda) &= \sum_{J=\frac{1}{2},\frac{3}{2}} H_{s_{\Lambda_b}, s_{\Lambda_J^*}}^{J_{\Lambda_J^*}} \times (D_{s_{\Lambda_J^*}, s_p}^{J_{\Lambda_J^*}}(0, \theta_\Lambda))^*, \\
H_{s_{\Lambda_b}, s_{\Lambda_J^*}}^{\frac{3}{2}} &= L_{\Lambda_{1520}^*}(M_{pK}^2, m_{\Lambda_J^*}) i\mathcal{M}(\Lambda_b \to \Lambda_{1520}^* J/\psi), \\
H_{s_{\Lambda_b}, s_{\Lambda_J^*}}^{\frac{1}{2}} &= L_{\Lambda_{1600}^*}(M_{pK}^2, m_{\Lambda_J^*}) i\mathcal{M}(\Lambda_b \to \Lambda_{1600}^* J/\psi) \\
&\quad + L_{\Lambda_{1800}^*}(M_{pK}^2, m_{\Lambda_J^*}) i\mathcal{M}(\Lambda_b \to \Lambda_{1800}^* J/\psi), \\
L_{\Lambda_J^*}(M_{pK}^2, m_{\Lambda_J^*}) &= \mathcal{A}_J \frac{1}{M_{pK}^2 - m_{\Lambda_J^*}^2 + im_{\Lambda_J^*}\Gamma_{\Lambda_J^*}}.
\end{aligned} \tag{11}
$$

The differential decay width is formulated as

$$
d\Gamma = d\Pi_4 \times \frac{(2\pi)^4}{2m_{\Lambda_b}} |\mathcal{M}(\Lambda_b \to \Lambda_J^*(pK)J/\psi(\ell^+ \ell^-))|^2, \tag{12}
$$

where the phase space is used as

$$
\begin{aligned}
&d\Pi_4(p_{\ell^+}, p_{\ell^-}, p_p, p_K) \\
&= (2\pi)^3 (2\pi)^3 dq^2 dM_{pK}^2 \times d\Pi_2(p_{\ell^+}, p_{\ell^-}) \times d\Pi_2(p_p, p_K) \\
&\quad \times d\Pi_2(p_{J/\psi}, p_{\Lambda_J^*}) \\
&= \frac{\sqrt{\lambda(m_{\Lambda_b}, m_{\Lambda_J^*}, q^2)}|\vec{p}_p|\sqrt{q^2 - 4m_\ell^2}}{(2\pi)^{10} \times 128\sqrt{q^2} m_{\Lambda_b}^2 \sqrt{M_{pK}^2}} \\
&\quad \times d\cos\theta d\cos\theta_\Lambda d\phi dM_{pK}^2 dq^2,
\end{aligned} \tag{13}
$$

with $|\vec{p}_p| = \sqrt{\lambda(m_{\Lambda_J^*}, m_K, m_p)}/(2m_{\Lambda_J^*})$, $\lambda(m_{\Lambda_J^*}, m_K, m_p) = ((m_{\Lambda_J^*} + m_K)^2 - m_p^2)((m_{\Lambda_J^*} - m_K)^2 - m_p^2)$, and $M_{pK}^2 = p_{\Lambda_J^*}^2$.

III. ANGULAR DISTRIBUTION OF $\Lambda_b \to \Lambda_J^*(pK)J/\psi(\ell^+\ell^-)$

Combining all the elements, one obtains the differential decay width for the four-body decay process $\Lambda_b \to \Lambda_J^*(pK)J/\psi(\ell^+\ell^-))$ as

$$\frac{d\Gamma(\Lambda_b \to \Lambda_J^*(pK)J/\psi(\ell^+\ell^-))}{d\cos\theta d\cos\theta_\Lambda d\phi dq^2 dM_{pK}^2} = \frac{\sqrt{\lambda(m_{\Lambda_b}, m_{\Lambda_J^*}, q^2)}|\vec{p}_p|}{8192\pi^6 m_{\Lambda_b}^3 m_{\Lambda_J^*}} \frac{1}{2} \sum_{s_{\Lambda_b}, s_p, s_+, s_-} \frac{3\pi\Gamma(J/\psi \to \ell^+\ell^-)m_{J/\psi}|L_{s_-,s_+}^{s_{J/\psi}}(\phi,\theta)\mathcal{A}_{s_p,s_{J/\psi}}^{s_{\Lambda_b}}(\theta_\Lambda)|^2}{(m_{J/\psi}^2 + 2m_\ell^2)|q^2 - m_{J/\psi}^2 + im_{J/\psi}\Gamma_{J/\psi}|^2}. \tag{14}$$

Using the narrow-width limit for the J/ψ,

$$\frac{\Gamma_{J/\psi} m_{J/\psi}}{|(q^2 - m_{J/\psi}^2) + im_{J/\psi}\Gamma_{J/\psi}|^2} = \pi\delta(q^2 - m_{J/\psi}^2), \tag{15}$$

one can arrive at the differential decay width as

$$\frac{d\Gamma(\Lambda_b \to \Lambda_J^*(pK)J/\psi(\ell^+\ell^-))}{d\cos\theta d\cos\theta_\Lambda d\phi dM_{pK}^2} = \frac{3\sqrt{\lambda(m_{\Lambda_b}, m_{\Lambda_J^*}, m_{J/\psi})}|\vec{p}_p|}{16384\pi^4 m_{\Lambda_b}^3 m_{\Lambda_J^*}(m_{J/\psi}^2 + 2m_\ell^2)} \frac{1}{2} \sum_{s_{\Lambda_b}, s_p, s_+, s_-} \mathcal{B}(J/\psi \to \ell^+\ell^-)|L_{s_-,s_+}^{s_{J/\psi}}(\phi,\theta)\mathcal{A}_{s_p,s_{J/\psi}}^{s_{\Lambda_b}}(\theta_\Lambda)|^2. \tag{16}$$

With the explicit expressions for $|L_{s_-,s_+}^{s_{J/\psi}}(\phi,\theta)\mathcal{A}_{s_p,s_{J/\psi}}^{s_{\Lambda_b}}(\theta_\Lambda)|^2$ given in the Appendix, the angular distribution is derived as

$$\frac{d\Gamma(\Lambda_b \to \Lambda_J^*(pK)J/\psi(\ell^+\ell^-))}{d\cos\theta d\cos\theta_\Lambda d\phi dM_{pK}^2} = \mathcal{P}(L_1 + L_2\cos 2\phi + L_3\cos 2\theta + L_4\sin 2\theta\cos\phi + L_5\cos 2\phi\cos 2\theta$$

$$+ L_6\sin 2\theta\sin\phi + L_7\sin 2\phi + L_8\cos 2\theta\sin 2\phi),$$

$$\mathcal{P} = \frac{3\sqrt{\lambda(m_{\Lambda_b}, m_{\Lambda_J^*}, m_{J/\psi})}|\vec{p}_p|}{8192\pi^4 m_{\Lambda_b}^3 m_{\Lambda_J^*}(1 + 2\hat{m}_\ell^2)}\mathcal{B}(J/\psi \to \ell^+\ell^-). \tag{17}$$

The angular coefficients $L_i(i = 1 - 8)$ are given as

$$L_1 = \sum_{s_{\Lambda_b}, s_p} \left(2\hat{m}_\ell^2(|\mathcal{A}_{s_p,-1}^{s_{\Lambda_b}}(\theta_\Lambda)|^2 + 2|\mathcal{A}_{s_p,0}^{s_{\Lambda_b}}(\theta_\Lambda)|^2 + |\mathcal{A}_{s_p,1}^{s_{\Lambda_b}}(\theta_\Lambda)|^2) + \frac{1}{2}(3|\mathcal{A}_{s_p,-1}^{s_{\Lambda_b}}(\theta_\Lambda)|^2 + 2|\mathcal{A}_{s_p,0}^{s_{\Lambda_b}}(\theta_\Lambda)|^2 + 3|\mathcal{A}_{s_p,1}^{s_{\Lambda_b}}(\theta_\Lambda)|^2) \right),$$

$$L_2 = -(4\hat{m}_\ell^2 - 1) \sum_{s_{\Lambda_b}, s_p} \mathcal{R}_e(\mathcal{A}_{s_p,-1}^{s_{\Lambda_b}}(\theta_\Lambda)\mathcal{A}_{s_p,1}^{s_{\Lambda_b}*}(\theta_\Lambda)),$$

$$L_3 = \frac{-1}{2}(4\hat{m}_\ell^2 - 1) \sum_{s_{\Lambda_b}, s_p} (|\mathcal{A}_{s_p,-1}^{s_{\Lambda_b}}(\theta_\Lambda)|^2 - 2|\mathcal{A}_{s_p,0}^{s_{\Lambda_b}}(\theta_\Lambda)|^2 + |\mathcal{A}_{s_p,1}^{s_{\Lambda_b}}(\theta_\Lambda)|^2),$$

$$L_4 = -\sqrt{2}(4\hat{m}_\ell^2 - 1) \sum_{s_{\Lambda_b}, s_p} \mathcal{R}_e(\mathcal{A}_{s_p,0}^{s_{\Lambda_b}}(\theta_\Lambda)(\mathcal{A}_{s_p,-1}^{s_{\Lambda_b}*}(\theta_\Lambda) - \mathcal{A}_{s_p,1}^{s_{\Lambda_b}*}(\theta_\Lambda))),$$

$$L_5 = (4\hat{m}_\ell^2 - 1) \sum_{s_{\Lambda_b}, s_p} \mathcal{R}_e(\mathcal{A}_{s_p,-1}^{s_{\Lambda_b}}(\theta_\Lambda)\mathcal{A}_{s_p,1}^{s_{\Lambda_b}*}(\theta_\Lambda)),$$

$$L_6 = -\sqrt{2}(4\hat{m}_\ell^2 - 1) \sum_{s_{\Lambda_b}, s_p} \mathcal{I}_m(\mathcal{A}_{s_p,0}^{s_{\Lambda_b}}(\theta_\Lambda)(\mathcal{A}_{s_p,-1}^{s_{\Lambda_b}*}(\theta_\Lambda) + \mathcal{A}_{s_p,1}^{s_{\Lambda_b}*}(\theta_\Lambda))),$$

$$L_7 = (4\hat{m}_\ell^2 - 1) \sum_{s_{\Lambda_b}, s_p} \mathcal{I}_m(\mathcal{A}_{s_p,-1}^{s_{\Lambda_b}}(\theta_\Lambda)\mathcal{A}_{s_p,1}^{s_{\Lambda_b}*}(\theta_\Lambda)) = -L_8. \tag{18}$$

Then one can explore the $L_i (i = 1-8)$ by expanding $\mathcal{A}_{s_p, s_{J/\psi}}^{s_{\Lambda_b}}$ which contain the resonance of $\Lambda_{1520,1600,1800}^*$. The specific expression including θ_Λ can be displayed in Appendix B. Thus, the differential decay width for $\Lambda_b \to \Lambda_J^*(pK^-)J/\psi(\ell^+\ell^-)$ as a function of θ_Λ, θ, ϕ, and M_{pK}^2 is given as

$$\frac{d\Gamma(\Lambda_b \to \Lambda_J^*(pK)J/\psi(\ell^+\ell^-))}{d\cos\theta d\cos\theta_\Lambda d\phi dM_{pK}^2} = \mathcal{P}(L_{11} + \cos\theta_\Lambda L_{12} + \cos 2\theta_\Lambda L_{13} + \cos 2\phi(L_{21} + \cos 2\theta_\Lambda L_{22})$$

$$+ \cos 2\theta(L_{31} + \cos\theta_\Lambda L_{32} + \cos 2\theta_\Lambda L_{33}) + \sin 2\theta \cos\phi(\sin\theta_\Lambda L_{41} + \sin 2\theta_\Lambda L_{42})$$

$$+ \cos 2\phi \cos 2\theta(L_{51} + \cos 2\theta_\Lambda L_{52}) + \sin 2\theta \sin\phi(\sin\theta_\Lambda L_{61} + \sin 2\theta_\Lambda L_{62})$$

$$+ \sin 2\phi(L_{71} + \cos 2\theta_\Lambda L_{72}) + \cos 2\theta \sin 2\phi(L_{81} + \cos 2\theta_\Lambda L_{82})). \tag{19}$$

Here the formulas of $L_{ij}(i = 1-8, j = 1-3)$ are also given in Appendix B.

IV. PHENOMENOLOGICAL APPLICATIONS

A. Transition form factors

The hadron matrix element $\langle \Lambda_J^* | \bar{s}\gamma^\mu(1-\gamma_5)b|\Lambda_b\rangle$ in Eq. (5) can be parametrized by form factors. For the $\Lambda_b \to \Lambda_{1520}^*$ transition, one can define the helicity-based form factors as [30]

$$\langle \Lambda_{1520}^*(p',s')|\bar{s}\gamma^\mu b|\Lambda_b(p,s)\rangle = \bar{u}_\lambda(p',s')\left(f_0^{3/2} \frac{m_{\Lambda_{1520}^*}}{s_{p+}} \frac{(m_{\Lambda_b} - m_{\Lambda_{1520}^*})p^\lambda q^\mu}{q^2} \right.$$

$$+ f_+^{3/2} \frac{m_{\Lambda_{1520}^*}}{s_{p-}} \frac{(m_{\Lambda_b} + m_{\Lambda_{1520}^*})p^\lambda(q^2(p^\mu + p'^\mu) - q^\mu(m_{\Lambda_b}^2 - m_{\Lambda_{1520}^*}^2))}{q^2 s_{p+}}$$

$$+ f_\perp^{3/2} \frac{m_{\Lambda_{1520}^*}}{s_{p-}} \left(p^\lambda \gamma^\mu - \frac{2p^\lambda(m_{\Lambda_b}p'^\mu + m_{\Lambda_{1520}^*}p^\mu)}{s_{p+}} \right)$$

$$\left. + f_{\perp'}^{3/2} \frac{m_{\Lambda_{1520}^*}}{s_{p-}} \left(p^\lambda \gamma^\mu - \frac{2p^\lambda p'^\mu}{m_{\Lambda_{1520}^*}} + \frac{2p^\lambda(m_{\Lambda_b}p'^\mu + m_{\Lambda_{1520}^*}p^\mu)}{s_{p+}} + \frac{s_{p-}g^{\lambda\mu}}{m_{\Lambda_{1520}^*}} \right) \right) u(p,s),$$

$$\langle \Lambda_{1520}^*(p',s')|\bar{s}\gamma^\mu \gamma_5 b|\Lambda_b(p,s)\rangle = \bar{u}_\lambda(p',s')\left(-g_0^{3/2}\gamma_5 \frac{m_{\Lambda_{1520}^*}}{s_{p-}} \frac{(m_{\Lambda_b} + m_{\Lambda_{1520}^*})p^\lambda q^\mu}{q^2} \right.$$

$$- g_+^{3/2}\gamma_5 \frac{m_{\Lambda_{1520}^*}}{s_{p+}} \frac{(m_{\Lambda_b} - m_{\Lambda_{1520}^*})p^\lambda(q^2(p^\mu + p'^\mu) - q^\mu(m_{\Lambda_b}^2 - m_{\Lambda_{1520}^*}^2))}{q^2 s_{p-}}$$

$$- g_\perp^{3/2}\gamma_5 \frac{m_{\Lambda_{1520}^*}}{s_{p+}} \left(p^\lambda \gamma^\mu - \frac{2p^\lambda(m_{\Lambda_b}p'^\mu - m_{\Lambda_{1520}^*}p^\mu)}{s_{p-}} \right)$$

$$\left. - g_{\perp'}^{3/2}\gamma_5 \frac{m_{\Lambda_{1520}^*}}{s_{p+}} \left(p^\lambda \gamma^\mu + \frac{2p^\lambda p'^\mu}{m_{\Lambda_{1520}^*}} + \frac{2p^\lambda(m_{\Lambda_b}p'^\mu + m_{\Lambda_{1520}^*}p^\mu)}{s_{p-}} - \frac{s_{p+}g^{\lambda\mu}}{m_{\Lambda_{1520}^*}} \right) \right) u(p,s), \tag{20}$$

with $q^\mu = p^\mu - p'^\mu$ being the transferred momentum and $s_{p\pm} = (m_{\Lambda_b} \pm m_{\Lambda_J^*})^2 - q^2$, $q^2 = m_{J/\psi}^2$.

These form factors have been calculated from lattice QCD (LQCD) [30], where multisets of lattice ensembles are used. To access the M_{pK}^2 distributions, the form factors are parametrized as [30]

$$f(M_{pK}^2) = F\left[1 + C\frac{m_\pi^2 - m_{\pi,\text{phys}}^2}{(4\pi f_\pi)^2} + Da^2\Lambda^2 \right] + A\left[1 + C'\frac{m_\pi^2 - m_{\pi,\text{phys}}^2}{(4\pi f_\pi)^2} + D'a^2\Lambda^2 \right](\omega - 1), \tag{21}$$

where the parameters F, A, C, D, C', and D' are fitted from the lattice data and $\omega = (m_{\Lambda_b}^2 + M_{pK}^2 - m_{J/\psi}^2)/2m_{\Lambda_b}m_{\Lambda_J^*}$. In the LQCD calculation, the finite lattice spacing and pion mass effects are also considered. In the physical pion limit $m_\pi = 135$ MeV and the continuum limit $a = 0$, and using $f_\pi = 132$, and $\Lambda = 300$ MeV, one can simplify the above parametrization as

$$f(M_{pK}^2) = F + A(\omega - 1). \qquad (22)$$

For the $\Lambda_b \to \Lambda_{1520}^*$ transition, results for the inputs F and A are shown in Table II, and in the following we will use these results as default.

If the final baryon is a spin-$\frac{1}{2}$ hadron, the weak transition form factor is parametrized as [31]

$$\langle \Lambda_J^*(p', s') | \bar{s} \gamma^\mu b | \Lambda_b(p, s) \rangle$$

$$= \bar{u}(p', s') \left(\gamma_\mu f_1^p + \frac{p_{\Lambda_b}^\mu}{m_{\Lambda_b}} f_2^p + \frac{p_{\Lambda_J^*}^\mu}{m_{\Lambda_J^*}} f_3^p \right) u(p, s),$$

$$\langle \Lambda_J^*(p', s') | \bar{s} \gamma^\mu \gamma_5 b | \Lambda_b(p, s) \rangle$$

$$= \bar{u}(p', s') \left(\gamma_\mu g_1^p + \frac{p_{\Lambda_b}^\mu}{m_{\Lambda_b}} g_2^p + \frac{p_{\Lambda_J^*}^\mu}{m_{\Lambda_J^*}} g_3^p \right) \gamma_5 u(p, s). \quad (23)$$

In Ref. [31], a model with a full quark model wave function and the full relativistic form of the quark is adopted to investigate the form factors, and these form factors are studied in the multicomponent numerical (MCN) model. The M_{pK}^2 dependence is parametrized as

$$f(M_{pK}^2) = (a_0 + a_2 p_\Lambda^2 + a_4 p_\Lambda^4) \exp\left(-\frac{6 m_q^2 p_\Lambda^2}{2 \tilde{m}_\Lambda^2 (\alpha_{\Lambda_b}^2 + \alpha_{\Lambda^*}^2)} \right). \qquad (24)$$

Here p_Λ represents one of the daughter baryon momenta in the Λ_b rest frame. The MCN model parameters a_0, a_2, and a_4 are given in Tables II and III, respectively. Because of the lack of results for the $\Lambda_b \to \Lambda_{1800}^*$ transition, we use the results for the $\Lambda_b \to \Lambda_{1405}^*$. This may induce sizable uncertainties, and future detailed analysis can resolve this approximation.

B. Numerical results

Two-body decays $\Lambda_b \to \Lambda_J^* J/\psi$ can provide a calibration for the four-body decay process, and the decay widths for $\Lambda_b \to \Lambda_J^* J/\psi$ are given as

$$\Gamma(\Lambda_b \to \Lambda_J^* J/\psi) = \sum_{s_{\Lambda_b}, s_{\Lambda_J^*}, s_{J/\psi}} \frac{|\vec{p}_{\Lambda_J^*}|}{8\pi m_{\Lambda_b}^2} \frac{1}{2} |\mathcal{M}(\Lambda_b \to \Lambda_J^* J/\psi)|^2. \qquad (25)$$

With the form factors from Ref. [31], one can calculate branching fractions for the process involving different resonances $\Lambda_{1520,1600,1800}^*$,

TABLE II. Input parameters in Eqs. (22) and (24) for Λ_{1520}^*.

Lattice QCD			MCN quark model			
Form factor	F	A	Form factor	a_0	a_2	a_4
$f_0^{3/2}$	3.54(29)	−14.7(3.3)	f_1	−1.66	−0.295	0.00924
$f_+^{3/2}$	0.0432(64)	1.63(19)	f_2	0.544	0.194	−0.00420
$f_\perp^{3/2}$	−0.068(18)	2.49(35)	f_3	0.126	0.00799	−0.000365
$f_{\perp'}^{3/2}$	0.0461(18)	−0.161(27)	f_4	−0.0330	−0.00977	0.00211
$g_0^{3/2}$	0.0024(38)	1.58(17)	g_1	−0.964	−0.100	0.00264
$g_+^{3/2}$	2.95(25)	−12.2(2.9)	g_2	0.625	0.219	−0.00508
$g_\perp^{3/2}$	2.92(24)	−11.8(2.8)	g_3	−0.183	−0.0380	0.00351
$g_{\perp'}^{3/2}$	−0.037(14)	0.09(25)	g_4	0.0530	0.0161	−0.00221
			$\alpha_{\Lambda_b} = 0.443$	$\alpha_{\Lambda^*(1520)} = 0.333$	$\tilde{m}_\Lambda = 1.1249$	$m_q = 0.2848$

TABLE III. Input parameters in Eqs. (22) and (24) for spin-1/2 resonance $\Lambda_{1600,1800}^*$ in MCN quark model.

Λ_{1600}^*				Λ_{1800}^*			
Form factor	a_0	a_2	a_4	Form factor	a_0	a_2	a_4
f_1^+	0.467	0.615	0.0568	f_1^-	0.246	0.238	0.00976
f_2^+	−0.381	−0.2815	−0.0399	f_2^-	−0.984	−0.0257	0.0173
f_3^+	0.0501	−0.0295	−0.00163	f_3^-	0.118	0.0237	−0.000692
g_1^+	0.114	0.300	0.0206	g_1^-	1.15	0.260	−0.00303
g_2^+	−0.394	−0.307	−0.0445	g_2^-	−0.874	−0.0264	0.0159
g_3^+	−0.0433	0.0478	0.00566	g_3^-	0.00871	−0.0196	−0.000997
	$\alpha_{\Lambda^*(1600)} = 0.387$				$\alpha_{\Lambda^*(1800)} = 0.333$		

$$\mathcal{B}(\Lambda_b \to \Lambda^*_{1520}J/\psi) = 5.78 \times 10^{-4},$$
$$\mathcal{B}(\Lambda_b \to \Lambda^*_{1600}J/\psi) = 2.44 \times 10^{-4},$$
$$\mathcal{B}(\Lambda_b \to \Lambda^*_{1800}J/\psi) = 4.48 \times 10^{-4}. \qquad (26)$$

There is no experimental measurement of the above three processes. However, the available data indicate $\mathcal{B}(\Lambda_b \to J/\psi\Lambda) \times \mathcal{B}(b \to \Lambda_b) = (5.8 \pm 0.8) \times 10^{-5}$ [32,33], where Λ is the ground state. Using the estimate of the fragmentation fraction $\mathcal{B}(b \to \Lambda_b) = 0.175 \pm 0.106$ [34], one can obtain $\mathcal{B}(\Lambda_b \to J/\psi\Lambda) = (3.3 \pm 0.5 \pm 2.0) \times 10^{-4}$, which is on the same order with the results in Eq. (26).

Based on the differential decay width in Eq. (17), one can obtain the differential decay width as

$$d\Gamma(\Lambda_b \to \Lambda^*_j(pK)J/\psi(\ell^+\ell^-))/dM^2_{pK}$$
$$= \mathcal{P}\frac{8\pi}{9}(9L_{11} - 3L_{13} - 3L_{31} + L_{33}). \qquad (27)$$

Using the inputs from the Particle Data Group [28],

$$\mathcal{B}(J/\psi \to e^+e^-) = (5.971 \pm 0.032)\%,$$
$$\mathcal{B}(J/\psi \to \mu^+\mu^-) = (5.961 \pm 0.033)\%,$$
$$\mathcal{B}(\Lambda^*_{1520} \to pK^-) = (22.5 \pm 0.5)\%,$$
$$\mathcal{B}(\Lambda^*_{1600} \to pK^-) \sim (10.5)\%, \quad \mathcal{B}(\Lambda^*_{1800} \to pK^-) \sim (16)\%,$$
$$\Gamma_{1520} = (0.01573 \pm 0.00026),$$
$$\Gamma_{1600} \sim \Gamma_{1800} \sim 0.2 \text{ GeV}, \quad m_p = 0.938 \text{ GeV},$$
$$m_K = 0.494 \text{ GeV}, \qquad (28)$$

one can obtain the Λ_b four-body decay widths with final state pK produced by a determined resonance $\Lambda^*_{1520,1600,1800}$ as

$$\mathcal{B}(\Lambda_b \to \Lambda^*(pK)J/\psi(\mu^+\mu^-)) = (1.35 \pm 0.28) \times 10^{-5},$$
$$\mathcal{B}(\Lambda_b \to \Lambda^*(pK)J/\psi(e^+e^-)) = (1.35 \pm 0.28) \times 10^{-5},$$
$$\mathcal{B}(\Lambda_b \to \Lambda^*_{1520}(pK)J/\psi(\mu^+\mu^-)) = (7.22 \pm 2.53) \times 10^{-6},$$
$$\mathcal{B}(\Lambda_b \to \Lambda^*_{1520}(pK)J/\psi(e^+e^-)) = (7.22 \pm 2.54) \times 10^{-6},$$
$$\mathcal{B}(\Lambda_b \to \Lambda^*_{1600}(pK)J/\psi(\mu^+\mu^-)) = 1.11 \times 10^{-6},$$
$$\mathcal{B}(\Lambda_b \to \Lambda^*_{1600}(pK)J/\psi(e^+e^-)) = 1.11 \times 10^{-6},$$
$$\mathcal{B}(\Lambda_b \to \Lambda^*_{1800}(pK)J/\psi(\mu^+\mu^-)) = 3.87 \times 10^{-6},$$
$$\mathcal{B}(\Lambda_b \to \Lambda^*_{1800}(pK)J/\psi(e^+e^-)) = 3.88 \times 10^{-6}. \qquad (29)$$

The $\Lambda_b \to \Lambda^*_{1600,1800}$ form factors are used from the MCN model [31], and no uncertainties are given. It is interesting to notice that such results are also in agreement with the results for two-body decays in the narrow-width approximation.

If the MCN model results for the $\Lambda_b \to \Lambda^*_{1520}$ form factors are used, we can find $\mathcal{B}(\Lambda_b \to \Lambda^*_{1520}(pK)J/\psi(\mu^+\mu^-)) = 1.904 \times 10^{-6}$, which is reduced by a factor
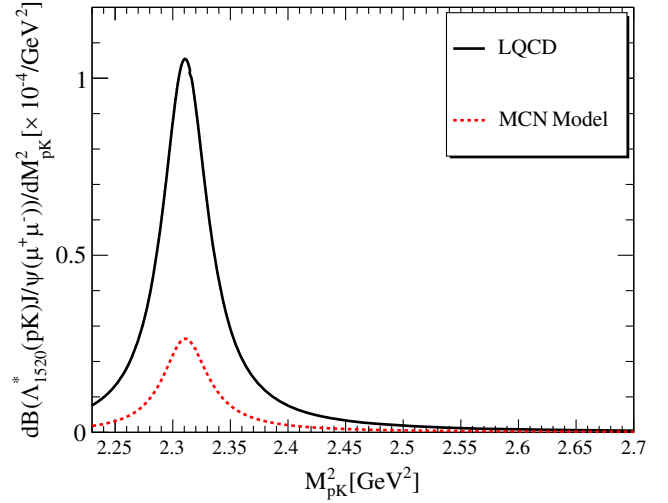
FIG. 2. The differential branching fraction $d\mathcal{B}/dM^2_{pK}$ for the process $\Lambda_b \to \Lambda^*_{1520}(pK)J/\psi(\ell^+\ell^-), \ell = \mu$ (in units of $10^{-4}/\text{GeV}^2$) with lattice QCD [30] and the MCN quark model [31] form factors.

of 3. In Fig. 2, we show the differential decay branching fraction $d\mathcal{B}/dq^2(\Lambda_b \to \Lambda^*_{1520}(pK)J/\psi(\ell^+\ell^-))$ with the two sets of form factors. It can be seen that a significant discrepancy appears at the low-M^2_{pK} region for different forms of parametrized form factors.

The differential decay widths for the processes $\Lambda_b \to \Lambda^*_j(pK^-)J/\psi(\ell^+\ell^-)$ as a function of M^2_{pK} are given in Fig. 3. We also show the normalized ϕ angular distribution for the Λ_b decay in Fig. 3. Since the lepton pair arises from the decay of J/ψ induced by vector current, angular distributions for the lepton are proportional to $\cos 2\theta$.

1. Distribution of θ_Λ

One can integrate the angle θ, ϕ and explore the normalized distribution of θ_Λ,

$$\frac{1}{\Gamma}d\Gamma(\Lambda_b \to \Lambda^*_j(pK)J/\psi(\ell^+\ell^-))/dM^2_{pK}d\cos\theta_\Lambda$$
$$= (L_\Lambda + L_{\Lambda c}\cos\theta_\Lambda + L_{\Lambda 2c}\cos 2\theta_\Lambda)/\Gamma, \qquad (30)$$

where

$$L_\Lambda = \mathcal{P}\frac{4\pi}{3}(3L_{11} - L_{31}), \qquad L_{\Lambda c} = \mathcal{P}\frac{4\pi}{3}(3L_{12} - L_{32}),$$
$$L_{\Lambda 2c} = \mathcal{P}\frac{4\pi}{3}(3L_{13} - L_{33}). \qquad (31)$$

The $\cos\theta_\Lambda$ distributions are described in Fig. 3. In the L_Λ all three resonances contribute, while the $\cos 2\theta_\Lambda$ term receives no contribution from spin-$\frac{1}{2}$ baryon and the $L_{\Lambda c}$
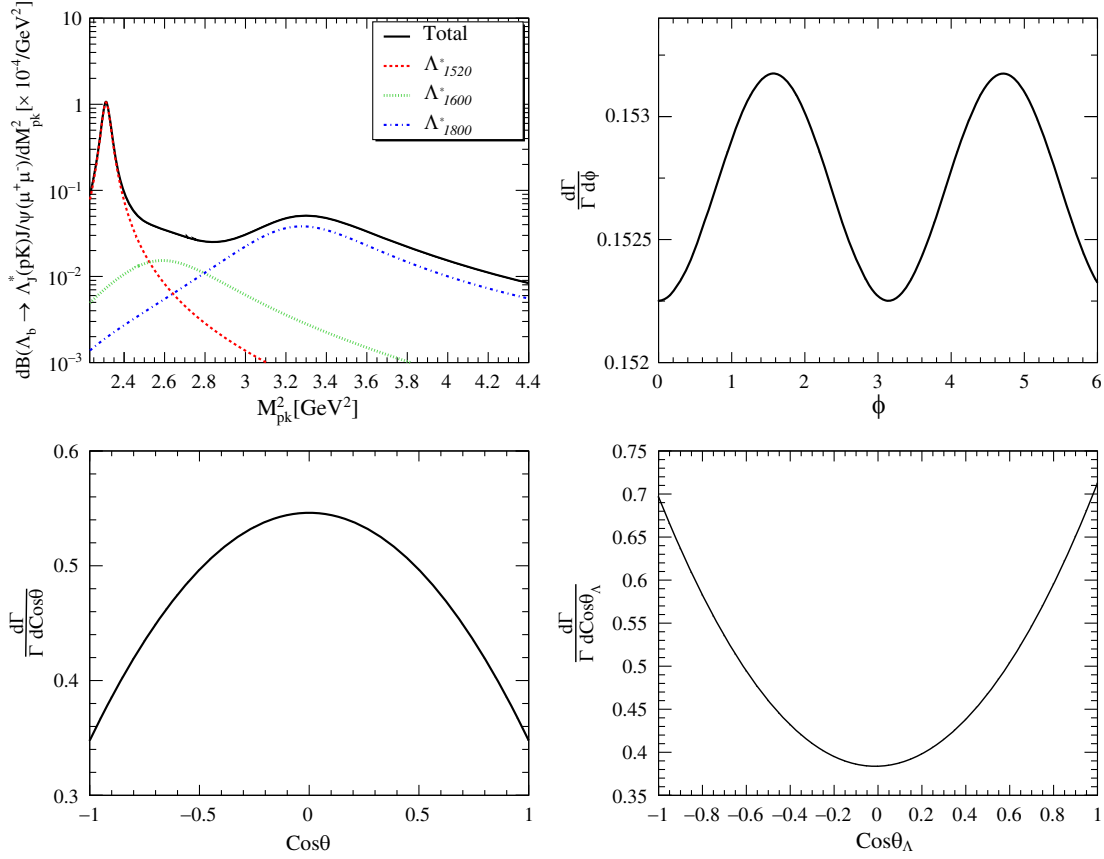
FIG. 3. The $(d\mathcal{B}/dM_{pK}^2, \frac{d\Gamma}{\Gamma d\phi}, \frac{d\Gamma}{\Gamma d\cos\theta}, \frac{d\Gamma}{\Gamma d\cos\theta_\Lambda})$ of process $\Lambda_b \to \Lambda^*(pK)J/\psi(\mu^+\mu^-)$.

corresponds to the interference of spin-$\frac{1}{2}$ and spin-$\frac{3}{2}$ resonance.

Based on this interference, one can construct a normalized forward-backward asymmetry A_{FB}^Λ of angle θ_Λ,

$$A_{\text{FB}}^\Lambda = \frac{[\int_0^1 - \int_{-1}^0]d\cos\theta_\Lambda \frac{d^2\Gamma}{dM_{pK}^2 d\cos\theta_\Lambda}}{[\int_0^1 + \int_{-1}^0]d\cos\theta_\Lambda \frac{d^2\Gamma}{dM_{pK}^2 d\cos\theta_\Lambda}}$$

$$= \frac{3(3L_{12} - L_{32})}{2(9L_{11} - 3L_{13} - 3L_{31} + L_{33})}$$

$$= \frac{3L_{\Lambda c}}{2(3L_\Lambda - L_{\Lambda 2c})}. \tag{32}$$

Results for A_{FB}^Λ are given in Fig. 4. It is interesting to notice that the forward-backward asymmetry has a crossing point, which satisfies

$$\frac{dA_{\text{FB}}^\Lambda}{dM_{pK}^2} \propto \frac{4\pi}{3}(3L_{12} - L_{32}) = 0, \tag{33}$$

or

$$\sum_{s_{\Lambda_b}, s_{\Lambda_J^*}=\pm\frac{1}{2}} (2\hat{m}_\ell^2 + 1)\mathcal{R}_e(H^{\frac{3}{2}}_{s_{\Lambda_b},s_{\Lambda_J^*}} H^{\frac{1}{2}*}_{s_{\Lambda_b},s_{\Lambda_J^*}})$$

$$= \sum_{s_{\Lambda_b}, s_{\Lambda_J^*}=\pm\frac{1}{2}} (2\hat{m}_\ell^2 + 1)(\mathcal{R}_e(H^{\frac{3}{2}}_{s_{\Lambda_b},s_{\Lambda_J^*}})\mathcal{R}_e(H^{\frac{1}{2}*}_{s_{\Lambda_b},s_{\Lambda_J^*}})$$

$$- \mathcal{I}_m(H^{\frac{3}{2}}_{s_{\Lambda_b},s_{\Lambda_J^*}})\mathcal{I}_m(H^{\frac{1}{2}*}_{s_{\Lambda_b},s_{\Lambda_J^*}})) = 0. \tag{34}$$
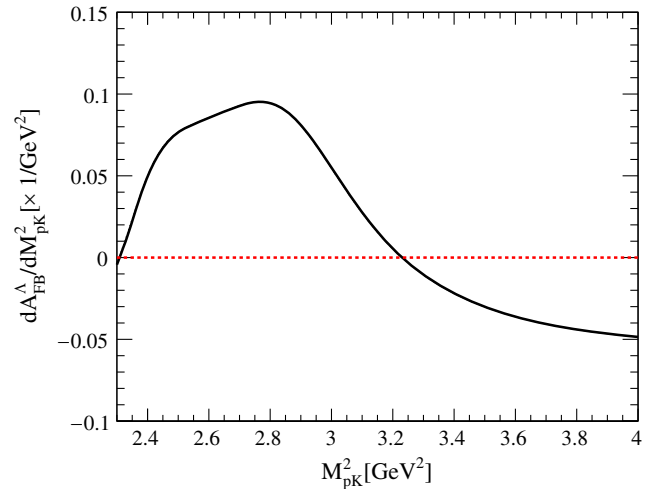
FIG. 4. The $dA_{\text{FB}}^\Lambda/dM_{pK}^2$ of process $\Lambda_b \to \Lambda_J^*(pK)J/\psi(\ell^+\ell^-)$ for $\ell = \mu$.

It can be seen from Fig. 4 that there are two cross points s_0^1 and s_0^2,

$$s_0^1 = 2.307 \text{ GeV}^2, \qquad s_0^2 = 3.231 \text{ GeV}^2. \qquad (35)$$

The two points are very close to the invariant mass square of $\Lambda^*_{1520,1800}$, $m^2_{\Lambda^*_{1520}} = 2.308 \text{ GeV}^2$, and $m^2_{\Lambda^*_{1800}} = 3.240 \text{ GeV}^2$. As shown in Fig. 3, the contribution of Λ^*_{1600} is tiny and can be neglected. Therefore, in this scenario, Eq. (34) becomes

$$\frac{dA^\Lambda_{FB}}{dM^2_{pK}} \propto \sum_{s_{\Lambda_b}, s_{\Lambda^*_J} = \pm\frac{1}{2}} (2\hat{m}^2_\ell + 1) \mathcal{R}_e(H^{\frac{3}{2}}_{s_{\Lambda_b}, s_{\Lambda^*_J}} H^{\frac{1}{2}*}_{s_{\Lambda_b}, s_{\Lambda^*_J}})$$

$$\propto \mathcal{R}_e(L_{\Lambda^*_{1520}} L_{\Lambda^*_{1800}}). \qquad (36)$$

The complex phase in $H^J_{s_{\Lambda_b}, s_{\Lambda^*_J}}$ comes from the line shape $L_{\Lambda^*_J}$, while the imaginary part is proportional to the $\Gamma_{\Lambda^*_J} m_{\Lambda^*_J}$. One can ignore the imaginary part, due to the small $\Gamma_{\Lambda^*_J}$. Thus, the forward-backward asymmetry will mostly be determined by line shape L_{Λ^*} and the equation becomes

$$\mathcal{R}_e(L_{\Lambda^*_{1520}} L^*_{\Lambda^*_{1800}}) \sim (M^2_{pK} - m^2_{\Lambda^*_{1520}})(M^2_{pK} - m^2_{\Lambda^*_{1800}}) = 0. \qquad (37)$$

Thus, the s_0^1 and s_0^2 should be close to the mass square of $\Lambda^*_{1520,1800}$. It will be a new method for precisely measuring resonant mass in experiments. In addition, one can find that the A^Λ_{FB} is positive in the region $M^2_{pK} = [s_0^1, s_0^2]$ and negative when M^2_{pK} is larger than s_0^2. Therefore, the two parts will almost cancel each other when the M^2_{pK} is integrated out in A^Λ_{FB}. The coefficient $L_{\Lambda c}$ in Eq. (30) has the same behavior with A^Λ_{FB} and it will also give a small value. This conclusion is also confirmed by our numerical analysis for integrating $L_{\Lambda c}$ with M^2_{pK} as
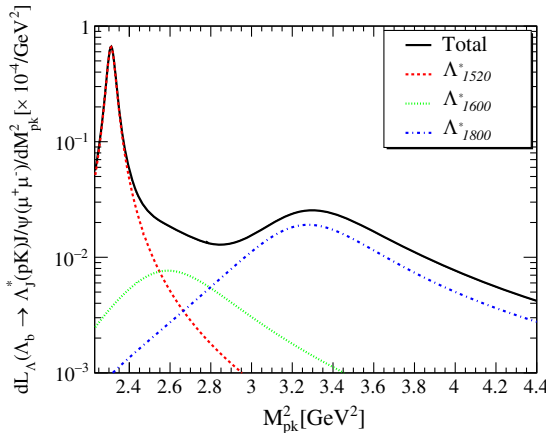
$$\int dM^2_{pK} L_{\Lambda c} = 1.95 \times 10^{-5}. \qquad (38)$$

Thus, Fig. 3 shows the nearly symmetric curve in $\cos\theta_\Lambda$ distribution. Additionally, we show the results for $(L_\Lambda, L_{\Lambda 2c})$ distributions in Fig. 5. It can be seen that only the spin-$\frac{3}{2}$ resonance contributes to the coefficient $L_{\Lambda 2c}$, and thus this angular coefficient gives a piece of clear information on the spin-$\frac{3}{2}$ resonance.

2. Distribution in the azimuthal angle ϕ

The normalized angular distribution in ϕ can be derived by integrating the angle (θ_Λ, θ),

$$\frac{1}{\Gamma} \frac{d^2\Gamma(\Lambda_b \to \Lambda^*_J(pK) J/\psi(\ell^+\ell^-))}{dM^2_{pK} d\phi}$$
$$= (L_\phi + L_{\phi 2c} \cos 2\phi + L_{\phi 2s} \sin 2\phi)/\Gamma, \qquad (39)$$

where

$$L_\phi = \mathcal{P}\frac{4}{9}(9L_{11} - (3L_{31} + 3L_{13}) + L_{33}),$$

$$L_{\phi 2c} = \mathcal{P}\frac{4}{9}(9L_{21} - (3L_{22} + 3L_{51}) + L_{52}),$$

$$L_{\phi 2s} = \mathcal{P}\frac{4}{9}(9L_{71} - (3L_{72} + 3L_{81}) + L_{82}). \qquad (40)$$

For these three coefficients, the numerical results $(L_\phi, L_{\phi 2c}, L_{\phi 2s})$ are given in Fig. 6. One can see that in Eq. (B2) only the interference of different polarization helicity amplitudes of Λ^*_{1520} can contribute to $L_{\phi 2s}$. Since the complex phase in the helicity amplitude comes from the Breit-Wigner line shape, the coefficients L_{71}, L_{72}, L_{81}, and L_{82} are equal to zero. Therefore, the coefficient $L_{\phi 2s}$ is vanishing.

We can see that L_ϕ has the same behavior as Eq. (17) and the numerical results of $L_{\phi 2c}$ are tiny, as shown in Fig. 6. Because the $\mathcal{R}_e(H^{\frac{3}{2}}_{\frac{1}{2},\frac{3}{2}} H^{\frac{3}{2}*}_{\frac{1}{2},-\frac{1}{2}})$ term in the coefficient L_{21}, L_{22}, L_{51}, and L_{52} are canceled with each other.
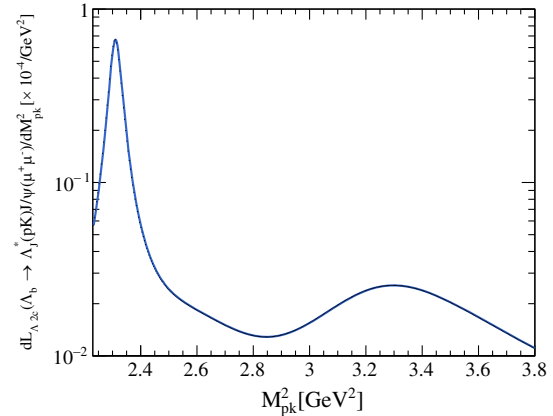
FIG. 5. The coefficients L_Λ and $L_{\Lambda 2c}$ in Eq. (30) for $\Lambda_b \to \Lambda^*(pK) J/\psi(\ell^+\ell^-)$, $\ell = \mu$.
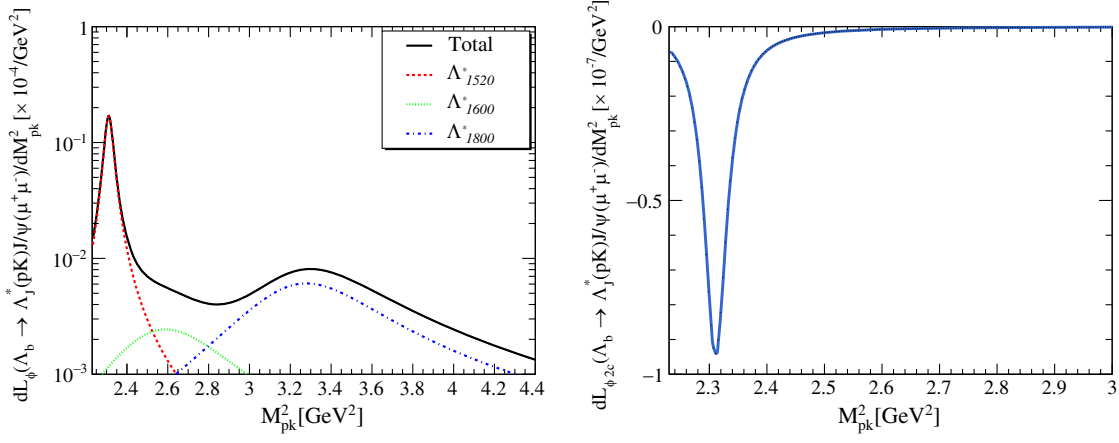
FIG. 6. The coefficients L_ϕ and $L_{2c\phi}$ in Eq. (6) for $\Lambda_b \to \Lambda_J^*(pK)J/\psi(\ell^+\ell^-)$, $\ell = \mu$, e.

3. Polarization of the Λ_b

The polarized angular distribution of s_{Λ_b} can be described as

$$
\frac{d\Gamma(s_{\Lambda_b})}{d\cos\theta d\cos\theta_\Lambda d\phi dM_{pK}^2} = \mathcal{P}(L_{11}^{(s_{\Lambda_b})} + \cos\theta_\Lambda L_{12}^{(s_{\Lambda_b})} + \cos 2\theta_\Lambda L_{13}^{(s_{\Lambda_b})} + \cos 2\phi (L_{21}^{(s_{\Lambda_b})} + \cos 2\theta_\Lambda L_{22}^{(s_{\Lambda_b})})
$$

$$
+ \cos 2\theta (L_{31}^{(s_{\Lambda_b})} + \cos\theta_\Lambda L_{32}^{(s_{\Lambda_b})} + \cos 2\theta_\Lambda L_{33}^{(s_{\Lambda_b})}) + \sin 2\theta \cos\phi (\sin\theta_\Lambda L_{41}^{(s_{\Lambda_b})} + \sin 2\theta_\Lambda L_{42}^{(s_{\Lambda_b})})
$$

$$
+ \cos 2\phi \cos 2\theta (L_{51}^{(s_{\Lambda_b})} + \cos 2\theta_\Lambda L_{52}^{(s_{\Lambda_b})}) + \sin 2\theta \sin\phi (\sin\theta_\Lambda L_{61}^{(s_{\Lambda_b})} + \sin 2\theta_\Lambda L_{62}^{(s_{\Lambda_b})})
$$

$$
+ \sin 2\phi (L_{71}^{(s_{\Lambda_b})} + \cos 2\theta_\Lambda L_{72}^{(s_{\Lambda_b})}) + \cos 2\theta \sin 2\phi (L_{81}^{(s_{\Lambda_b})} + \cos 2\theta_\Lambda L_{82}^{(s_b)})). \tag{41}
$$

Using the polarized distribution, the normalized polarized decay width can be defined as

$$
\frac{dN_{\Gamma_P}}{dM_{pK}^2} = \frac{\frac{d\Gamma(\frac{1}{2})}{dM_{pK}^2} - \frac{d\Gamma(-\frac{1}{2})}{dM_{pK}^2}}{\frac{d\Gamma(\frac{1}{2})}{dM_{pK}^2} + \frac{d\Gamma(-\frac{1}{2})}{dM_{pK}^2}}, \tag{42}
$$

and it is shown for the LQCD form factor and MCN quark model in Fig. 7.

The distribution of normalized polarized decay width shows a discrepancy with different polarized Λ_b. The distributions of normalized polarized branching fractions with two sets of form factors are shown in Fig. 7, which indicates the distribution of the two types of methods are similar, except in the low-M_{pK}^2 region. After normalizing the polarized decay width, the difference caused by LQCD and MCN form factors is less significant. This is because, in the normalized decay width, many common factors have been canceled. In addition, one can also find that the branching fraction with $s_{\Lambda_b} = 1/2$ is larger than that with $s_{\Lambda_b} = -1/2$ in the low-M_{pK}^2 region for both of the two sets of form factor results. One can see that the decay width in Eq. (19) shows the symmetry of transformation $((s_{\Lambda_b}, s_{\Lambda_j^*}) \to (-s_{\Lambda_b}, -s_{\Lambda_j^*}))$. Since the helicity amplitudes in Appendix A show that for vector current and axis vector

current the transformation brings positive and negative signs, respectively, the polarized decay width is mainly contributed to by the interference of vector current and axis vector current hadron helicity amplitudes. It is noteworthy
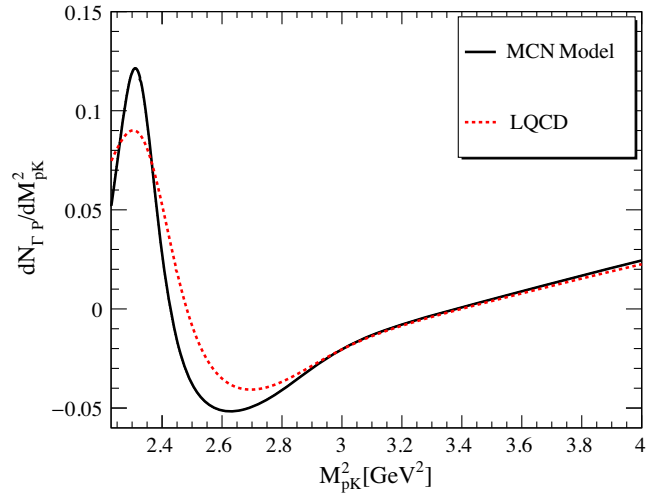
FIG. 7. The normalized polarized decay width dN_{Γ_P}/dM_{pK}^2 of $\Lambda_b(s_{\Lambda_b}) \to \Lambda_J^*(pK)J/\psi(\mu^+\mu^-)$. The black solid line utilizes the MCN quark model form factors and the red dotted one is drawn by LQCD form factors for resonance Λ_{1520}^* and the MCN quark model form factors for $\Lambda_{1600,1800}^*$.

that the interference terms between vector current and axis vector current helicity amplitudes have no contributions to the nonpolarized decay width. Therefore, the polarized decay width is a very important and unique observable for the study of the hadron matrix element structure.

V. CONCLUSIONS

In this work, the differential and integrated decay width for the process of $\Lambda_b \rightarrow \Lambda_J^*(pK)J/\psi(\ell^+\ell^-)$ through different resonances $\Lambda^*(\frac{1}{2}^+, \frac{1}{2}^-, \frac{3}{2}^-)$ are studied. Branching fractions with the individual resonances and total results are given in Eq. (29) by taking form factors of $\Lambda_b \rightarrow \Lambda_{1520}^*$ in lattice QCD and form factors of $\Lambda_b \rightarrow \Lambda_{1600,1800}^*$ in the MCN quark model.

For this process, we have derived the angular distribution with the possible resonance $\Lambda_{1520,1600,1800}^*$ and other phenomenological results, such as partial decay width, polarization, and forward-backward asymmetry with final states as muon and electron, respectively. Our results with different lepton e and μ are highly consistent with the lepton flavor universality. It has a good reference value for lepton flavor universal experiments. For the resonance Λ_{1520}^*, we adopt different types of form factors: the lattice QCD and MCN quark model, which shows a big discrepancy in the low-M_{pK}^2 region in Fig. 2. Since the lattice QCD has more reasonable results only in the high-M_{pK}^2 region,

we give the branching fraction and differential branching fractions for both of the two sets of form factors. We have analyzed the distribution of the angle and show the dependence of M_{pK}^2.

Results in this work will serve as a calibration for the study of $b \rightarrow s\bar{\mu}\mu$ decays in Λ_b decays in the future and provide useful information toward the understanding of the properties of the Λ_J^* baryons. Recently, the LHCb Collaboration has analyzed the process $\Lambda_b \rightarrow pK^-\ell^+\ell^-$ [24]. Therefore, the analysis of the angular distribution of $\Lambda_b \rightarrow \Lambda_J^*(pK)J/\psi(\ell^+\ell^-)$ in the LHCb is feasible and we urge our experimental colleagues to analyze this very interesting process.

ACKNOWLEDGMENTS

APPENDIX A: HELICITY AMPLITUDE

The hadronic helicity amplitudes we used are defined with the hadron matrix element as

$$H_A(s_1, s_2, s_W) = \langle \Lambda_J^*(p', s_2)|\bar{s}\gamma^\mu\gamma_5 b|\Lambda_b(p, s_1)\rangle \epsilon_\mu^*(q, s_W),$$
$$H_V(s_1, s_2, s_W) = \langle \Lambda_J^*(p', s_2)|\bar{s}\gamma^\mu b|\Lambda_b(p, s_1)\rangle \epsilon_\mu^*(q, s_W). \tag{A1}$$

We give the hadronic helicity amplitudes for the $\Lambda_b \rightarrow \Lambda_{1520}^*$ transition,

$$H_V\left(s_1 = \frac{1}{2}, s_2 = \frac{3}{2}, s_W = 1\right) = H_V\left(s_1 = -\frac{1}{2}, s_2 = -\frac{3}{2}, s_W = -1\right) = -f_4(M_{pk}^2)\sqrt{s_{p+}}, \tag{A2}$$

$$H_V\left(s_1 = \frac{1}{2}, s_2 = -\frac{1}{2}, s_W = -1\right) = H_V\left(s_1 = -\frac{1}{2}, s_2 = \frac{1}{2}, s_W = 1\right) = \sqrt{\frac{s_{p+}}{3}}\left(\frac{s_{p-}}{m_\Lambda m_{\Lambda_{1520}^*}}f_1(M_{pk}^2) - f_4(M_{pk}^2)\right), \tag{A3}$$

$$H_V\left(s_1 = \frac{1}{2}, s_2 = \frac{1}{2}, s_W = 0\right) = H_V\left(s_1 = -\frac{1}{2}, s_2 = -\frac{1}{2}, s_W = 0\right)$$
$$= \sqrt{\frac{s_{p+}}{6}}\frac{1}{m_{J/\psi}}\left[s_{p-}s_{p+}\left(\frac{f_1(M_{Pk}^2)}{s_{p+}}\left(\frac{1}{m_{\Lambda_{1520}^*}} + \frac{1}{m_{\Lambda_b}}\right) + f_2(M_{Pk}^2)\frac{1}{2m_{\Lambda_{1520}^*}m_{\Lambda_b}^2}\right.\right.$$
$$\left.\left. + f_3(M_{Pk}^2)\frac{1}{2m_{\Lambda_{1520}^*}m_{\Lambda_b}\sqrt{M_{pk}^2}}\right) + f_4(M_{Pk}^2)\frac{m_{\Lambda_b}^2 - m_{J/\psi}^2 - M_{pk}^2}{m_{\Lambda_{1520}^*}}\right], \tag{A4}$$

$$H_A\left(s_1 = \frac{1}{2}, s_2 = \frac{3}{2}, s_W = 1\right) = -H_A\left(s_1 = -\frac{1}{2}, s_2 = -\frac{3}{2}, s_W = -1\right) = g_4(M_{Pk}^2)\sqrt{s_{p-}}, \tag{A5}$$

$$H_A\left(s_1 = \frac{1}{2}, s_2 = -\frac{1}{2}, s_W = -1\right) = -H_A\left(s_1 = -\frac{1}{2}, s_2 = \frac{1}{2}, s_W = 1\right) = \sqrt{\frac{s_{p-}}{3}}\left(\frac{s_{p+}}{m_{\Lambda_{1520}^*} m_{\Lambda_b}} g_1(M_{Pk}^2) - g_4(M_{Pk}^2)\right), \quad \text{(A6)}$$

$$H_A\left(s_1 = \frac{1}{2}, s_2 = \frac{1}{2}, s_W = 0\right) = -H_A\left(s_1 = -\frac{1}{2}, s_2 = -\frac{1}{2}, s_W = 0\right)$$

$$= \sqrt{\frac{s_{p-}}{6}}\frac{1}{m_{J/\psi}}\left[s_{p-}s_{p+}\left(\frac{g_1(M_{Pk}^2)}{s_{p-}}\left(\frac{1}{m_{\Lambda_{1520}^*}} - \frac{1}{m_{\Lambda_b}}\right)\right.\right.$$

$$\left.- g_2(M_{Pk}^2)\frac{1}{2m_{\Lambda_{1520}^*} m_{\Lambda_b}^2} - g_3(M_{Pk}^2)\frac{1}{2m_{\Lambda_{1520}^*} m_{\Lambda_b}\sqrt{M_{pk}^2}}\right)$$

$$+ g_4(M_{Pk}^2)\frac{-m_{\Lambda_b}^2 + m_{J/\psi}^2 + M_{pk}^2}{m_{\Lambda_{1520}^*}}\right]. \quad \text{(A7)}$$

If the spin of the final state is one-half, the helicity amplitude is given as

$$H_V\left(s_1 = -\frac{1}{2}, s_2 = \frac{1}{2}, s_W = 1\right) = H_V\left(s_1 = \frac{1}{2}, s_2 = -\frac{1}{2}, s_W = -1\right) = \sqrt{2}[f_1(M_{pK}^2)\sqrt{s_{p-}}], \quad \text{(A8)}$$

$$H_V\left(s_1 = \frac{1}{2}, s_2 = \frac{1}{2}, s_W = 0\right) = H_V\left(s_1 = -\frac{1}{2}, s_2 = -\frac{1}{2}, s_W = 0\right)$$

$$= \frac{\sqrt{s_{p-}}}{m_{J/\psi}}\left[(m_{\Lambda_b} + m_{\Lambda_j^*})f_1(M_{pK}^2) + \frac{s_{p+}}{2m_{\Lambda_b}}f_2(M_{pK}^2) + f_3\frac{s_{p+}}{2\sqrt{M_{pK}^2}}\right],$$

$$H_A\left(s_1 = -\frac{1}{2}, s_2 = \frac{1}{2}, s_W = 1\right) = -H_A\left(s_1 = \frac{1}{2}, s_2 = -\frac{1}{2}, s_W = -1\right)$$

$$= \sqrt{2s_{p+}}[g_1(M_{pK}^2))], \quad \text{(A9)}$$

$$H_A\left(s_1 = \frac{1}{2}, s_2 = \frac{1}{2}, s_W = 0\right) = -H_A\left(s_1 = -\frac{1}{2}, s_2 = -\frac{1}{2}, s_W = 0\right)$$

$$= \frac{\sqrt{s_{p+}}}{m_{J/\psi}}\left[(-m_{\Lambda_b} + m_{\Lambda_j^*})g_1(M_{pK}^2) + \frac{s_{p-}}{2m_{\Lambda_b}}g_2(M_{pK}^2) + g_3\frac{s_{p-}}{2\sqrt{M_{pK}^2}}\right]. \quad \text{(A10)}$$

The leptonic helicity amplitudes $L_{s_-,s_+}^{s_{J/\psi}}$ are

$$L_{\frac{1}{2},\frac{1}{2}}^{1}(\phi,\theta) = L_{-\frac{1}{2},-\frac{1}{2}}^{1}(\phi,\theta) = -i\sqrt{2}m_\ell e^{-i\phi}\sin\theta, \qquad L_{\frac{1}{2},-\frac{1}{2}}^{1}(\phi,\theta) = -i\frac{m_{J/\psi}}{\sqrt{2}}m_\ell e^{-i\phi}(\cos\theta + 1),$$

$$L_{-\frac{1}{2},\frac{1}{2}}^{1}(\phi,\theta) = i\frac{m_{J/\psi}}{\sqrt{2}}m_\ell e^{-i\phi}(\cos\theta - 1), \qquad L_{\frac{1}{2},\frac{1}{2}}^{0}(\phi,\theta) = L_{-\frac{1}{2},-\frac{1}{2}}^{0}(\phi,\theta) = -2im_\ell\cos\theta,$$

$$L_{-\frac{1}{2},-\frac{1}{2}}^{-1}(\phi,\theta) = L_{-\frac{1}{2},-\frac{1}{2}}^{-1}(\phi,\theta) = i\sqrt{2}m_\ell e^{i\phi}\sin\theta, \qquad L_{-\frac{1}{2},\frac{1}{2}}^{-1}(\phi,\theta) = -i\frac{m_{J/\psi}}{\sqrt{2}}m_\ell e^{i\phi}(\cos\theta + 1),$$

$$L_{\frac{1}{2},-\frac{1}{2}}^{-1}(\phi,\theta) = i\frac{m_{J/\psi}}{\sqrt{2}}m_\ell e^{i\phi}(\cos\theta - 1). \quad \text{(A11)}$$

For the $J = \frac{1}{2}$ resonances Λ_J^*, the Wigner functions are

$$D_{\frac{1}{2},\frac{1}{2}}^{\frac{1}{2}}(\phi_\Lambda,\theta_\Lambda) = e^{-i\frac{1}{2}\phi_\Lambda}\cos\left(\frac{1}{2}\theta_\Lambda\right), \qquad D_{\frac{1}{2},-\frac{1}{2}}^{\frac{1}{2}}(\phi_\Lambda,\theta_\Lambda) = -e^{-i\frac{1}{2}\phi_\Lambda}\sin\left(\frac{1}{2}\theta_\Lambda\right),$$

$$D_{-\frac{1}{2},\frac{1}{2}}^{\frac{1}{2}}(\phi_\Lambda,\theta_\Lambda) = e^{-i\frac{1}{2}\phi_\Lambda}\sin\left(\frac{1}{2}\theta_\Lambda\right), \qquad D_{-\frac{1}{2},-\frac{1}{2}}^{\frac{1}{2}}(\phi_\Lambda,\theta_\Lambda) = e^{-i\frac{1}{2}\phi_\Lambda}\cos\left(\frac{1}{2}\theta_\Lambda\right). \quad \text{(A12)}$$

For the $J = \frac{3}{2}$ resonances Λ_J^*, the Wigner functions are

$$D_{\frac{3}{2},\frac{1}{2}}^{\frac{1}{2}}(\phi_\Lambda,\theta_\Lambda) = -\sqrt{3}e^{-i\frac{3}{2}\phi_\Lambda}\frac{1+\cos\theta_\Lambda}{2}\sin\left(\frac{1}{2}\theta_\Lambda\right), \qquad D_{\frac{3}{2},-\frac{1}{2}}^{\frac{1}{2}}(\phi_\Lambda,\theta_\Lambda) = \sqrt{3}e^{-i\frac{3}{2}\phi_\Lambda}\frac{1-\cos\theta_\Lambda}{2}\cos\left(\frac{1}{2}\theta_\Lambda\right),$$

$$D_{\frac{1}{2},\frac{1}{2}}^{\frac{1}{2}}(\phi_\Lambda,\theta_\Lambda) = e^{-i\frac{1}{2}\phi_\Lambda}\frac{3\cos\theta_\Lambda-1}{2}\cos\left(\frac{1}{2}\theta_\Lambda\right), \qquad D_{\frac{1}{2},-\frac{1}{2}}^{\frac{1}{2}}(\phi_\Lambda,\theta_\Lambda) = -e^{-i\frac{1}{2}\phi_\Lambda}\frac{3\cos\theta_\Lambda+1}{2}\sin\left(\frac{1}{2}\theta_\Lambda\right),$$

$$D_{-\frac{3}{2},-\frac{1}{2}}^{\frac{1}{2}}(\phi_\Lambda,\theta_\Lambda) = \sqrt{3}e^{i\frac{3}{2}\phi_\Lambda}\frac{1+\cos\theta_\Lambda}{2}\sin\left(\frac{1}{2}\theta_\Lambda\right), \qquad D_{\frac{3}{2},-\frac{1}{2}}^{\frac{1}{2}}(\phi_\Lambda,\theta_\Lambda) = \sqrt{3}e^{i\frac{3}{2}\phi_\Lambda}\frac{1-\cos\theta_\Lambda}{2}\cos\left(\frac{1}{2}\theta_\Lambda\right),$$

$$D_{-\frac{1}{2},-\frac{1}{2}}^{\frac{1}{2}}(\phi_\Lambda,\theta_\Lambda) = e^{i\frac{1}{2}\phi_\Lambda}\frac{3\cos\theta_\Lambda-1}{2}\cos\left(\frac{1}{2}\theta_\Lambda\right), \qquad D_{-\frac{1}{2},\frac{1}{2}}^{\frac{1}{2}}(\phi_\Lambda,\theta_\Lambda) = e^{i\frac{1}{2}\phi_\Lambda}\frac{3\cos\theta_\Lambda+1}{2}\sin\left(\frac{1}{2}\theta_\Lambda\right). \tag{A13}$$

APPENDIX B: COEFFICIENT FUNCTION IN ANGULAR DISTRIBUTION

The specific expressions of coefficient L_i in containing the resonance $\Lambda_{1520,1600,1800}^*$ are

$$L_1 = \sum_{s_p}((4\hat{m}_\ell^2+1)(|H_{\frac{1}{2},\frac{1}{2}}^{\frac{1}{2}}D_{\frac{1}{2},s_p}^{\frac{1}{2}}(0,\theta_\Lambda)|^2 + |H_{\frac{1}{2},\frac{1}{2}}^{\frac{3}{2}}D_{\frac{1}{2},s_p}^{\frac{3}{2}}(0,\theta_\Lambda)|^2 + 2\mathcal{R}_e(H_{\frac{1}{2},\frac{1}{2}}^{\frac{1}{2}}H_{\frac{1}{2},\frac{1}{2}}^{\frac{3}{2}*})D_{\frac{1}{2},s_p}^{\frac{1}{2}*}(0,\theta_\Lambda)D_{\frac{1}{2},s_p}^{\frac{3}{2}}(0,\theta_\Lambda))$$

$$+\frac{1}{2}(4\hat{m}_\ell^2+3)(|H_{\frac{1}{2},-\frac{1}{2}}^{\frac{1}{2}}D_{-\frac{1}{2},s_p}^{\frac{1}{2}}(0,\theta_\Lambda)|^2 + |H_{\frac{1}{2},-\frac{1}{2}}^{\frac{3}{2}}D_{-\frac{1}{2},s_p}^{\frac{3}{2}}(0,\theta_\Lambda)|^2 + |H_{\frac{1}{2},\frac{3}{2}}^{\frac{3}{2}}D_{\frac{3}{2},s_p}^{\frac{3}{2}}(0,\theta_\Lambda)|^2$$

$$+2\mathcal{R}_e(H_{\frac{1}{2},-\frac{1}{2}}^{\frac{1}{2}}H_{\frac{1}{2},-\frac{1}{2}}^{\frac{3}{2}*})D_{-\frac{1}{2},s_p}^{\frac{1}{2}*}(0,\theta_\Lambda)D_{-\frac{1}{2},s_p}^{\frac{3}{2}}(0,\theta_\Lambda))) + ((s_{\Lambda_b},s_{\Lambda_J^*}) \to (-s_{\Lambda_b},-s_{\Lambda_J^*})),$$

$$L_2 = -(4\hat{m}_\ell^2-1)\sum_{s_p}\sum_{J=\frac{1}{2},\frac{3}{2}}\mathcal{R}_e(H_{\frac{1}{2},-\frac{1}{2}}^{J}H_{\frac{1}{2},\frac{3}{2}}^{\frac{3}{2}*})D_{-\frac{1}{2},s_p}^{*J}(0,\theta_\Lambda)D_{\frac{3}{2},s_p}^{\frac{3}{2}}(0,\theta_\Lambda) + ((s_{\Lambda_b},s_{\Lambda_J^*}) \to (-s_{\Lambda_b},-s_{\Lambda_J^*})),$$

$$L_3 = \frac{-1}{2}(4\hat{m}_\ell^2-1)\sum_{s_p}(|H_{\frac{1}{2},-\frac{1}{2}}^{\frac{1}{2}}D_{-\frac{1}{2},s_p}^{\frac{1}{2}}(0,\theta_\Lambda)|^2 + |H_{\frac{1}{2},-\frac{1}{2}}^{\frac{3}{2}}D_{-\frac{1}{2},s_p}^{\frac{3}{2}}(0,\theta_\Lambda)|^2$$

$$+2\mathcal{R}_e(H_{\frac{1}{2},-\frac{1}{2}}^{\frac{1}{2}}H_{\frac{1}{2},-\frac{1}{2}}^{\frac{3}{2}*})D_{-\frac{1}{2},s_p}^{\frac{1}{2}*}(0,\theta_\Lambda)D_{-\frac{1}{2},s_p}^{\frac{3}{2}}(0,\theta_\Lambda) - 4\mathcal{R}_e(H_{\frac{1}{2},\frac{1}{2}}^{\frac{1}{2}}H_{\frac{1}{2},\frac{1}{2}}^{\frac{3}{2}*})D_{\frac{1}{2},s_p}^{\frac{1}{2}*}(0,\theta_\Lambda)D_{\frac{1}{2},s_p}^{\frac{3}{2}}(0,\theta_\Lambda),$$

$$+|H_{\frac{1}{2},\frac{3}{2}}^{\frac{3}{2}}D_{\frac{3}{2},s_p}^{\frac{3}{2}}(0,\theta_\Lambda)|^2 - 2|H_{\frac{1}{2},\frac{1}{2}}^{\frac{1}{2}}D_{\frac{1}{2},s_p}^{\frac{1}{2}}(0,\theta_\Lambda)|^2 - 2|H_{\frac{1}{2},\frac{1}{2}}^{\frac{3}{2}}D_{\frac{1}{2},s_p}^{\frac{3}{2}}(0,\theta_\Lambda)|^2) + ((s_{\Lambda_b},s_{\Lambda_J^*}) \to (-s_{\Lambda_b},-s_{\Lambda_J^*})),$$

$$L_4 = -\sqrt{2}(4\hat{m}_\ell^2-1)\sum_{s_p}\sum_{J,J'=\frac{1}{2},\frac{3}{2}}(\mathcal{R}_e(H_{\frac{1}{2},\frac{1}{2}}^{J}H_{\frac{1}{2},-\frac{1}{2}}^{*J'})D_{\frac{1}{2},s_p}^{*J}(0,\theta_\Lambda)D_{-\frac{1}{2},s_p}^{J'}(0,\theta_\Lambda)$$

$$-\mathcal{R}_e(H_{\frac{1}{2},\frac{1}{2}}^{J}H_{\frac{1}{2},\frac{3}{2}}^{\frac{3}{2}*})D_{\frac{1}{2},s_p}^{*J}(0,\theta_\Lambda)D_{\frac{3}{2},s_p}^{\frac{3}{2}}(0,\theta_\Lambda)) - ((s_{\Lambda_b},s_{\Lambda_J^*}) \to (-s_{\Lambda_b},-s_{\Lambda_J^*})),$$

$$L_5 = -L_2,$$

$$L_6 = -\sqrt{2}(4\hat{m}_\ell^2-1)\sum_{s_p}\sum_{J,J'=\frac{1}{2},\frac{3}{2}}(\mathcal{I}_m(H_{\frac{1}{2},\frac{1}{2}}^{J}H_{\frac{1}{2},-\frac{1}{2}}^{*J'})D_{\frac{1}{2},s_p}^{*J}(0,\theta_\Lambda)D_{-\frac{1}{2},s_p}^{J'}(0,\theta_\Lambda)$$

$$+\mathcal{I}_m(H_{\frac{1}{2},\frac{1}{2}}^{J}H_{\frac{1}{2},\frac{3}{2}}^{\frac{3}{2}*})D_{\frac{1}{2},s_p}^{*J}(0,\theta_\Lambda)D_{\frac{3}{2},s_p}^{\frac{3}{2}}(0,\theta_\Lambda)) + ((s_{\Lambda_b},s_{\Lambda_J^*}) \to (-s_{\Lambda_b},-s_{\Lambda_J^*})),$$

$$L_7 = (4\hat{m}_\ell^2-1)\sum_{s_p}\sum_{J=\frac{1}{2},\frac{3}{2}}\mathcal{I}_m(H_{\frac{1}{2},-\frac{1}{2}}^{J}H_{\frac{1}{2},\frac{3}{2}}^{\frac{3}{2}*})D_{-\frac{1}{2},s_p}^{*J}(0,\theta_\Lambda)D_{\frac{3}{2},s_p}^{\frac{3}{2}}(0,\theta_\Lambda) - ((s_{\Lambda_b},s_{\Lambda_J^*}) \to (-s_{\Lambda_b},-s_{\Lambda_J^*})),$$

$$L_8 = -L_7. \tag{B1}$$

Here both J and J' represent the spin of resonant state Λ_J^*.

The formulas of coefficient function $L_{ij}(i = 1 - 8, j = 1 - 3)$ are given as

$$L_{11} = \frac{1}{4}\hat{m}_\ell^2(3|H^{\frac{3}{2}}_{\frac{1}{2},\frac{3}{2}}|^2 + 16|H^{\frac{1}{2}}_{\frac{1}{2},\frac{1}{2}}|^2 + 10|H^{\frac{3}{2}}_{\frac{1}{2},\frac{1}{2}}|^2 + 5|H^{\frac{1}{2}}_{\frac{1}{2},-\frac{1}{2}}|^2 + 8|H^{\frac{1}{2}}_{\frac{1}{2},-\frac{1}{2}}|^2)$$

$$+ \frac{1}{16}(9|H^{\frac{3}{2}}_{\frac{1}{2},\frac{3}{2}}|^2 + 16|H^{\frac{1}{2}}_{\frac{1}{2},\frac{1}{2}}|^2 + 10|H^{\frac{3}{2}}_{\frac{1}{2},\frac{1}{2}}|^2 + 15|H^{\frac{3}{2}}_{\frac{1}{2},-\frac{1}{2}}|^2 + 24|H^{\frac{1}{2}}_{\frac{1}{2},-\frac{1}{2}}|^2) + ((s_{\Lambda_b}, s_{\Lambda_J^*}) \to (-s_{\Lambda_b}, -s_{\Lambda_J^*})),$$

$$L_{12} = 2(4\hat{m}_\ell^2 + 1)\mathcal{R}_e(H^{\frac{3}{2}}_{\frac{1}{2},\frac{1}{2}}H^{\frac{1}{2}*}_{\frac{1}{2},\frac{1}{2}}) + (4\hat{m}_\ell^2 + 3)\mathcal{R}_e(H^{\frac{3}{2}}_{-\frac{1}{2},\frac{1}{2}}H^{\frac{1}{2}*}_{-\frac{1}{2},\frac{1}{2}}) + ((s_{\Lambda_b}, s_{\Lambda_J^*}) \to (-s_{\Lambda_b}, -s_{\Lambda_J^*})),$$

$$L_{13} = \frac{3}{16}((4\hat{m}_\ell^2 + 1)2|H^{\frac{3}{2}}_{\frac{1}{2},\frac{1}{2}}|^2 + (4\hat{m}_\ell^2 + 3)(|H^{\frac{3}{2}}_{\frac{1}{2},-\frac{1}{2}}|^2 - |H^{\frac{3}{2}}_{\frac{1}{2},\frac{3}{2}}|^2)) + ((s_{\Lambda_b}, s_{\Lambda_J^*}) \to (-s_{\Lambda_b}, -s_{\Lambda_J^*})),$$

$$L_{21} = \frac{\sqrt{3}}{8}(4\hat{m}_\ell^2 - 1)\mathcal{R}_e(H^{\frac{3}{2}}_{\frac{1}{2},\frac{3}{2}}H^{\frac{3}{2}*}_{\frac{1}{2},-\frac{1}{2}}) + ((s_{\Lambda_b}, s_{\Lambda_J^*}) \to (-s_{\Lambda_b}, -s_{\Lambda_J^*})),$$

$$L_{22} = -L_{21},$$

$$L_{31} = \frac{-1}{16}(4\hat{m}_\ell^2 - 1)(3|H^{\frac{3}{2}}_{\frac{1}{2},\frac{3}{2}}|^2 - 10|H^{\frac{3}{2}}_{\frac{1}{2},\frac{1}{2}}|^2 - 16|H^{\frac{1}{2}}_{\frac{1}{2},\frac{1}{2}}|^2 + 5|H^{\frac{3}{2}}_{\frac{1}{2},-\frac{1}{2}}|^2 + 8|H^{\frac{1}{2}}_{\frac{1}{2},-\frac{1}{2}}|^2) + ((s_{\Lambda_b}, s_{\Lambda_J^*}) \to (-s_{\Lambda_b}, -s_{\Lambda_J^*})),$$

$$L_{32} = -(4\hat{m}_\ell^2 - 1)(\mathcal{R}_e(H^{\frac{3}{2}}_{-\frac{1}{2},\frac{1}{2}}H^{\frac{1}{2}*}_{-\frac{1}{2},\frac{1}{2}}) - 2\mathcal{R}_e(H^{\frac{3}{2}}_{\frac{1}{2},\frac{1}{2}}H^{\frac{1}{2}*}_{\frac{1}{2},\frac{1}{2}})) + ((s_{\Lambda_b}, s_{\Lambda_J^*}) \to (-s_{\Lambda_b}, -s_{\Lambda_J^*})),$$

$$L_{33} = \frac{3}{16}(4\hat{m}_\ell^2 - 1)(|H^{\frac{3}{2}}_{\frac{1}{2},\frac{3}{2}}|^2 + 2|H^{\frac{3}{2}}_{\frac{1}{2},\frac{1}{2}}|^2 - |H^{\frac{3}{2}}_{\frac{1}{2},-\frac{1}{2}}|^2) + ((s_{\Lambda_b}, s_{\Lambda_J^*}) \to (-s_{\Lambda_b}, -s_{\Lambda_J^*})),$$

$$L_{41} = \frac{-\sqrt{2}}{2}(4\hat{m}_\ell^2 - 1)(\sqrt{3}\mathcal{R}_e(H^{\frac{3}{2}}_{\frac{1}{2},\frac{3}{2}}H^{\frac{1}{2}*}_{\frac{1}{2},\frac{1}{2}}) + \mathcal{R}_e(H^{\frac{3}{2}}_{\frac{1}{2},-\frac{1}{2}}H^{\frac{1}{2}*}_{\frac{1}{2},\frac{1}{2}}) - \mathcal{R}_e(H^{\frac{3}{2}}_{-\frac{1}{2},-\frac{1}{2}}H^{\frac{1}{2}*}_{-\frac{1}{2},\frac{1}{2}})) + ((s_{\Lambda_b}, s_{\Lambda_J^*}) \to (-s_{\Lambda_b}, -s_{\Lambda_J^*})),$$

$$L_{42} = \frac{-1}{2\sqrt{2}}(4\hat{m}_\ell^2 - 1)(\sqrt{3}\mathcal{R}_e(H^{\frac{3}{2}}_{\frac{1}{2},\frac{3}{2}}H^{\frac{3}{2}*}_{\frac{1}{2},\frac{1}{2}})) + ((s_{\Lambda_b}, s_{\Lambda_J^*}) \to (-s_{\Lambda_b}, -s_{\Lambda_J^*})),$$

$$L_{51} = -L_{21} = -L_{52},$$

$$L_{61} = \frac{1}{\sqrt{2}}(4\hat{m}_\ell^2 - 1)(\mathcal{I}_m(H^{\frac{3}{2}}_{\frac{1}{2},-\frac{1}{2}}H^{\frac{1}{2}*}_{\frac{1}{2},\frac{1}{2}}) + \mathcal{I}_m(H^{\frac{3}{2}}_{\frac{1}{2},\frac{1}{2}}H^{\frac{1}{2}*}_{\frac{1}{2},-\frac{1}{2}}) - \sqrt{3}\mathcal{I}_m(H^{\frac{3}{2}}_{\frac{1}{2},\frac{3}{2}}H^{\frac{1}{2}*}_{\frac{1}{2},\frac{1}{2}})) - ((s_{\Lambda_b}, s_{\Lambda_J^*}) \to (-s_{\Lambda_b}, -s_{\Lambda_J^*})),$$

$$L_{62} = \frac{1}{2\sqrt{2}}(4\hat{m}_\ell^2 - 1)(\sqrt{3}\mathcal{I}_m(H^{\frac{3}{2}}_{\frac{1}{2},\frac{1}{2}}H^{\frac{3}{2}*}_{\frac{1}{2},\frac{3}{2}})) - ((s_{\Lambda_b}, s_{\Lambda_J^*}) \to (-s_{\Lambda_b}, -s_{\Lambda_J^*})),$$

$$L_{71} = \frac{\sqrt{3}}{8}(4\hat{m}_\ell^2 - 1)((\mathcal{I}_m(H^{\frac{3}{2}}_{\frac{1}{2},-\frac{1}{2}}H^{\frac{3}{2}*}_{\frac{1}{2},\frac{3}{2}}))) + ((s_{\Lambda_b}, s_{\Lambda_J^*}) \to (-s_{\Lambda_b}, -s_{\Lambda_J^*})),$$

$$L_{72} = L_{81} = -L_{82} = -L_{71}. \tag{B2}$$

APPENDIX C: THE J/ψ DECAY PROCESS $J/\psi \to \ell^+\ell^+$

The F^*F type interaction is parametrized as

$$\mathcal{H}_{\text{eff}} = gF^{\mu\nu}F'_{\mu\nu}, \tag{C1}$$

which gives amplitude for $J/\psi \to \bar{\ell}\ell$ as

$$i\mathcal{M}(J/\psi \to \ell^+\ell^-) = \langle \ell^+(s_+)\ell^-(s_-)| - igF^{\mu\nu}F'_{\mu\nu}(0)|J/\psi(s_{J/\psi})\rangle$$

$$= \langle \ell^+(s_+)\ell^-(s_-)| - igF^{\mu\nu}F'_{\mu\nu}(0)\left(-ie\int d^4x \bar{\ell}\gamma^\rho \ell A_\rho(x)\right)|J/\psi(s_{J/\psi})\rangle$$

$$= -2eg\int \frac{d^4q}{(2\pi)^4}q^2\int d^4x e^{ix(p_{\ell^+}+p_{\ell^-}-q)}\frac{-i}{q^2} \times \bar{u}(s_-)\gamma^\mu v(s_+)\epsilon_\mu(s_{J/\psi})$$

$$= 2ieg \times \bar{u}(s_-)\gamma^\mu v(s_+)\epsilon_\mu(s_{J/\psi}). \tag{C2}$$

The $\gamma_\mu \cdot A^\mu$ type Hamiltonian is given as

$$\mathcal{H}_{\text{eff}} = g_1 \bar{\ell} \gamma^\mu \ell A'_\mu. \tag{C3}$$

The amplitude for $J/\psi \to \bar{\ell}\ell$ becomes

$$
\begin{aligned}
&i\mathcal{M}(J/\psi \to \ell^+\ell^-) \\
&= \langle \ell^+(s_+)\ell^-(s_-)| - ig_1 \bar{\ell}\gamma^\mu \ell A'_\mu(0)|J/\psi(s_{J/\psi})\rangle \\
&= -ig_1 \times \bar{u}(s_-)\gamma^\mu v(s_+)\epsilon_\mu(s_{J/\psi}). \tag{C4}
\end{aligned}
$$

Comparing the amplitudes derived by two different types of Hamiltonian, one can find a relation between the coupling constant g and g_1 as

$$g = \frac{-g_1}{2e}. \tag{C5}$$

It shows that the two parametrizations are equivalent.

[1] S. K. Choi *et al.* (Belle Collaboration), Phys. Rev. Lett. **91,** 262001 (2003).
[2] K. Abe *et al.* (Belle Collaboration), Phys. Rev. Lett. **94,** 182002 (2005).
[3] B. Aubert *et al.* (*BABAR* Collaboration), Phys. Rev. D **71,** 071103 (2005).
[4] R. Aaij *et al.* (LHCb Collaboration), Phys. Rev. Lett. **115,** 072001 (2015).
[5] R. Aaij *et al.* (LHCb Collaboration), Sci. Bull. **66,** 1278 (2021).
[6] R. Aaij *et al.* (LHCb Collaboration), Phys. Rev. Lett. **122,** 222001 (2019).
[7] A. J. Buras and M. Munz, Phys. Rev. D **52,** 186 (1995).
[8] J. T. Wei *et al.* (Belle Collaboration), Phys. Rev. Lett. **103,** 171801 (2009).
[9] X. G. He and S. Oh, J. High Energy Phys. 09 (2009) 027.
[10] Z. P. Xing and Z. X. Zhao, Phys. Rev. D **98,** 056002 (2018).
[11] Z. X. Zhao, Eur. Phys. J. C **78,** 756 (2018).
[12] T. Huber, T. Hurth, J. Jenkins, E. Lunghi, Q. Qin, and K. K. Vos, J. High Energy Phys. 10 (2019) 228.
[13] T. Huber, T. Hurth, J. Jenkins, E. Lunghi, Q. Qin, and K. K. Vos, J. High Energy Phys. 10 (2020) 088.
[14] F. Munir Bhutta, Z. R. Huang, C. D. Lü, M. A. Paracha, and W. Wang, Nucl. Phys. **B979,** 115763 (2022).
[15] X. Q. Li, M. Shen, D. Y. Wang, Y. D. Yang, and X. B. Yuan, Nucl. Phys. **B980,** 115828 (2022).
[16] X. G. He and G. Valencia, Phys. Lett. B **821,** 136607 (2021).
[17] J. Y. Cen, Y. Cheng, X. G. He, and J. Sun, Nucl. Phys. **B978,** 115762 (2022).
[18] Y. S. Li, S. P. Jin, J. Gao, and X. Liu, arXiv:2210.04640.
[19] J. P. Lees *et al.* (*BABAR* Collaboration), Phys. Rev. Lett. **109,** 101802 (2012).
[20] S. Wehle *et al.* (Belle Collaboration), Phys. Rev. Lett. **118,** 111801 (2017).
[21] R. Aaij *et al.* (LHCb Collaboration), J. High Energy Phys. 08 (2017) 055.
[22] R. Aaij *et al.* (LHCb Collaboration), Phys. Rev. Lett. **115,** 111803 (2015); **115,** 159901(E) (2015).
[23] R. Aaij *et al.* (LHCb Collaboration), J. High Energy Phys. 09 (2018) 146.
[24] R. Aaij *et al.* (LHCb Collaboration), J. High Energy Phys. 05 (2020) 040.
[25] R. Aaij *et al.* (LHCb Collaboration), J. High Energy Phys. 11 (2021) 043.
[26] R. Aaij *et al.* (LHCb Collaboration), Nat. Phys. **18,** 277 (2022).
[27] R. Aaij *et al.* (LHCb Collaboration), Phys. Rev. D **105,** 012010 (2022).
[28] R. L. Workman *et al.* (Particle Data Group), Prog. Theor. Exp. Phys. **2022,** 083C01 (2022).
[29] G. Buchalla, A. J. Buras, and M. E. Lautenbacher, Rev. Mod. Phys. **68,** 1125 (1996).
[30] S. Meinel and G. Rendon, Phys. Rev. D **105,** 054511 (2022).
[31] L. Mott and W. Roberts, Int. J. Mod. Phys. A **27,** 1250016 (2012).
[32] V. M. Abazov *et al.* (D0 Collaboration), Phys. Rev. D **84,** 031102 (2011).
[33] F. Abe *et al.* (CDF Collaboration), Phys. Rev. D **55,** 1142 (1997).
[34] Y. K. Hsiao, P. Y. Lin, L. W. Luo, and C. Q. Geng, Phys. Lett. B **751,** 127 (2015).